Chapter 4

Hybrid Energy Systems for Combined Cooling, Heating, and Power and Hydrogen Production Based on Solar Energy: A Techno-Economic Analysis

Nan Li and Yujia Song

December 2021

This chapter should be cited as

Li, Nan and Y. Song (2021), 'Hybrid Energy Systems for Combined Cooling, Heating, and Power and Hydrogen Production Based on Solar Energy: A Techno-Economic Analysis', in Li, Y., H. Phoumin, and S. Kimura (eds.), *Hydrogen Sourced from Renewables and Clean Energy: A Feasibility Study of Achieving Large-scale Demonstration.* ERIA Research Project Report FY2021 No. 19, Jakarta: ERIA, pp.51-93.

Chapter 4

Hybrid Energy Systems for Combined Cooling, Heating, and Power and Hydrogen Production Based on Solar Energy: A Techno-Economic Analysis

Nan Li and Yujia Song

In this chapter, solar energy, the hydrogen production system and the combined cooling, heating, and power (CCHP) system are combined to realise cooling–heating–power hydrogen multi-generation. Taking the total cost as the objective function, the configurations of the system with the lowest unit energy supply cost is obtained. The simulation work of the hybrid system based upon public buildings in Dalian, China is carried out to find an appropriate design scheme. The optimal system is analysed and described in detail. The results show when the daily hydrogen production is 700 kilograms (kg), the unit energy cost is the lowest, which is $0.0615/kilowatt hours (kWh). The total cost of the system is about $3.49 million and the annual carbon dioxide emissions of the system is about 8,570 tons. The fossil energy consumption of the system is about 42,100 megawatt hours (MWh). Therefore, 700 kg/day hydrogen supply is the best choice from the economic point of view. By comparing the total cost, carbon dioxide emissions and primary energy consumption with three existing systems, it is concluded that this system performs the best in three aspects.

Keywords: Hydrogen production; solar energy; combined cooling, heating, and power; total cost; carbon dioxide emissions; fossil energy consumption

1. Project Basis

1.1. Background

With the rapid development of the economy and the continuous consumption of fossil energy, the realisation of low-carbon and environmental protection development has become the goal of the power generation industry of all countries in the world. The new energy generation technologies have become the development direction of the power industry. Amongst them, wind power and photovoltaic (PV) power generation, due to their superior natural resource endowment, rapid development, and flexible installation, are more mature and more efficient than other new energy power generation technologies. They can well replace fossil energy power generation. According to statistics, the world's PV installed capacity grew rapidly from 2010 to 2012 and the growth rate has gradually slowed. At the end of 2016, the global PV installed capacity was about 76 gigawatts (GW), with the cumulative installed capacity exceeding 300 GW. Amongst them, China, the United States, and Japan ranked the top three with 34.54 GW, 14.1 GW, and 8.6 GW, respectively. From the perspective of regional distribution, Asia is still the world's

most important PV power generation market, and China, the United States, and India have a strong driving force for PV power generation industry development.

Despite the rapid development of China's renewable energy, there are also shortcomings. Wind energy and PV are easily affected by seasons, climate, and time, which can lead to unstable power output of new energy systems. Grid connection will have a great impact on the voltage and stability of the power grid. The phenomenon of wind and PV power curtailment is still prominent in China. In 2019, China's wind and light abandonment capacity was16.9 billion kWh and 4.6 billion kWh, with a total of more than 20 billion kWh. Therefore, how to effectively use renewable energy and reduce wind and photovoltaic power curtailment has great significance to improve the utilisation rate of renewable energy and promote the energy revolution in China. With the rapid development of society, great importance has been attached to the efficient and clean power generation technology of renewable energy (wind energy and solar energy) and widely used by countries all over the world. Wind power generation and PV power generation are the main forms of renewable energy utilisation. Their rapid and large-scale development makes it difficult for the power grid to absorb the electricity.

To develop PV power generation more widely, two major problems need to be solved. The first problem is due to the instability of photovoltaic power generation which will have a greater impact on the grid. In order to avoid this impact, the grid will not accept unstable electricity, which will cause a waste of power. The second problem is the difficulty in storing energy from PV power generation. Traditional electrochemical energy storage, electromagnetic energy storage, and physical energy storage technologies cannot meet the needs of massive energy storage and the development of pure green energy in the future. Green storage is one of the key problems to solve the difficulty of connecting wind power and PV power.

Pumped storage and compressed air storage are relatively mature technical schemes, but they are limited by specific conditions, such as a large amount of water, reasonable terrain, dependence on fossil fuels, etc. The electrochemical battery is another way, but in the short term, lead-acid batteries, nickel-metal hydride batteries, lithium-ion batteries, or all-vanadium REDOX flow batteries will be limited by cost, scale, and technology maturity. Other energy storage methods such as flywheel energy storage cannot readily meet the challenge of large-scale application due to their low efficiency and small capacity. As a clean energy source, hydrogen has the characteristics of high energy density, large capacity, long life, and easy storage and transmission. It has become one of the optimal plans for large-scale comprehensive green development, storage, and utilisation of wind power and PV power. Using electrolysis of water to produce hydrogen for energy storage, PV power generation can integrate hydrogen as a clean and high-energy fuel into the existing gas supply network to realise the complementary conversion of electricity to gas. It can also be directly and efficiently used. Especially with the development of efficient and clean technologies such as fuel cells, hydrogen generation by PV power generation can provide clean hydrogen fuel for fuel cell vehicles and form them into green energy vehicles in the true sense.

To achieve ‘the peak of China's carbon dioxide emissions by 2030, and strive to achieve carbon neutrality by 2060’, the government requires traditional enterprises to offset their carbon dioxide emissions in the form of energy conservation and emissions reduction, to achieve zero emissions of carbon dioxide. Therefore, traditional enterprises have a strong desire to invest in the construction of clean energy power generation projects to balance carbon dioxide emissions. However, due to a large number of light-discarding phenomena in northeast China, the government controls the clean energy power generation to prevent a large number of wind and light-discarding phenomena. Therefore, the combined use of light-discarding and distributed energy can realise the combined supply of cold, heat, electricity, and hydrogen, which not only solves the problem of carbon neutralisation of traditional enterprises but also solves the problem of light discarding for the government. In this chapter, the solar energy, hydrogen production system and CCHP system are combined to realise the system of the cold–heat–electricity–hydrogen combined power supply. Taking the total system cost as the objective function, the configuration of the system with the lowest unit energy supply cost is obtained. The optimal system is analysed and described in detail. When the daily hydrogen supply is 700 kg, the unit energy cost is the lowest, which is $0.0615/kWh. The total cost of the system is $3,491,080, and the annual carbon dioxide emission of the system is 8,574,791 kg. The primary energy consumption of the system is 42,135,860 kWh. Therefore, from the economic point of view, 700 kg/day hydrogen supply is the best choice. By comparing the total cost, carbon dioxide emissions, and primary energy consumption with the three reference systems, it is concluded that the CCHP system performs the best in three aspects.

In recent years, China's primary energy consumption structure has been dominated by traditional fossil fuel energy represented by coal and oil, which causes serious problems of energy security and environmental pollution. Therefore, it is imperative to promote energy reform and develop ‘green, low-carbon, clean, efficient, and safe’ energy technology. By the end of 2019, the installed capacity of renewable energy power generation in China was 794 million kW, accounting for 39.5% of the total power capacity, including 210 million kW of wind power and 204 million kW of PV power generation. At the same time, distributed energy has also been vigorously developed due to its environmental protection and flexibility. From 2015 to 2019, the cumulative installed capacity of distributed photovoltaic power generation in China has increased year by year, reaching 50.6 GW in 2018. By the first three quarters of 2019, the cumulative installed capacity of distributed PV power generation in China had reached 58.7 GW. Despite the rapid development of renewable energy in China, there are still some shortcomings. Wind energy and light energy are easily affected by the seasons, climate, and time, which leads to the instability of the output power of the new energy system. If the grid is connected, the voltage and stability of the power grid will be greatly affected. At present, the phenomenon of ‘abandoning wind’ and ‘abandoning light’ is still prominent in China. In 2019, China's abandoned wind power was 16.9 billion kWh, and the abandoned light power was 4.6 billion kWh, with a total of more than 20 billion kWh. Therefore, how to effectively use renewable energy and reduce the rate of abandoned wind and light power

is of significance to improve the utilisation rate of renewable energy and promote the energy revolution.

The task of national energy conservation and emissions reduction is important, which is related to the people's livelihoods. There is an urgent need to control air pollution. In the coming years, the task of controlling air pollution in provinces and cities will be a challenge, forcing governments at all levels to address their responsibilities and strive to achieve energy conservation and emissions reduction targets. The development of renewable energy has become an important measure to achieve energy conservation and emissions reduction. As one of the renewable energy sources, solar energy is also a key field of development.

At present, domestic and foreign scholars generally believe that hydrogen technology is an important part and key technical support of renewable energy systems and the energy internet. As the most ideal energy carrier and clean energy internationally recognised, hydrogen is known as 'the ultimate energy of the 21st century'. Today, with the increasingly serious problems of environmental pollution and greenhouse gas emissions, hydrogen energy has become the focus of the international community with its unique advantages of high heat and being clean and efficient. We need to reach a consensus on development. The 973 and 863 plans of the Ministry of Science and Technology have funded several plans on hydrogen energy. Local governments have issued policies on the hydrogen energy industry, and Sichuan, Guangdong, Beijing, Shanghai, Tianjin, amongst others, have implemented nearly 20 projects. How to use hydrogen energy efficiently to solve the increasingly serious problems of energy security and environmental pollution has become the current research focus.

Due to the serious problem of light discarding in China, the national government wants to reduce the light discarding rate of PV power generation. If the problem of the light discarding rate cannot be solved, the government will no longer approve the investment and construction of new energy power generation projects to prevent the increase of the light discarding rate. On the other hand, China will enhance its national independent contribution and adopt more powerful policies and measures to achieve the peak of carbon dioxide emissions by 2030 and achieve carbon neutrality by 2060. The government requires traditional enterprises to offset their carbon dioxide emissions by energy conservation and emissions reduction, to achieve zero emissions of carbon dioxide. Therefore, traditional enterprises have a strong desire to invest in the construction of clean energy power generation projects to balance the carbon dioxide emissions and reduce the pressure of survival. To solve the problem of carbon neutralisation in traditional enterprises, and at the same time to prevent a large number of new energy projects from abandoning light, we use the excess electricity generated by PV power generation for the CCHP system. In this system, the electricity generated by PV cells is used to supply power for the community, and the surplus electricity is converted into hydrogen through the proton exchange membrane electrolyser to provide hydrogen for the community or for electric cars. The purpose of this study is to optimise the scale of the proposed combined cooling, heating, power, and hydrogen supply system to meet the

load requirements of selected buildings. This, in turn, will reduce electricity purchases from the grid by increasing building self-sufficiency, lower energy costs, and lower peak load limits.

1.2. Literature Review

Hydrogen as a new way of energy storage, combined with wind and PV will improve the utilization rate of power generation. In remote areas (weak power grid system), conventional energy cannot guarantee the quality of the power supply and the investment is high. As a multi-purpose energy carrier, hydrogen has obvious advantages such as heat, electricity, and hydrogen generation, and the integrated construction of pure green energy vehicles in hydrogen refuelling stations, which can effectively solve the above problems.

The production and utilisation of hydrogen energy are attracting the attention of many scholars and research institutions all over the world. The comprehensive analysis of the current research situation in China and abroad shows that the utilisation of electrolytic aquatic hydrogen is a good way to improve energy efficiency. Scholars have conducted a large number of studies on energy cost optimisation, net cost optimisation, system reliability, economy, optimal system configuration, optimisation algorithm, and optimal system scheduling of hydrogen energy systems. Ma, Yang, and Lu (2014) obtained the optimal solar wind battery system configuration by calculating the optimal net cost and energy cost, and analysed and described the optimal system in detail. Javed and Ma (2019) estimated the scale of a hybrid solar–wind battery system based on energy cost and system reliability. A genetic algorithm is used to optimise the proposed system, and the results are compared with those of the Homer Pro software. Singh, Baredar, and Gupta (2017) proposed hydrogen fuel cell and solar PV hybrid energy systems for independent application. Through the fuzzy logic method to calculate the best equipment cost and replacement cost, and the best equipment cost is applied to the Homer Pro software to calculate the best performance of the hybrid energy system. Singh, Chauhan, and Singh (2020) conducted technical and economic analysis on the hybrid energy system based on the solar PV fuel cell. Artificial bee colony algorithms, particle swarm optimisation algorithms, and hybrid algorithms were used to optimise the net cost of the proposed system. The results of the three algorithms are compared in terms of cost effectiveness. Mokhtara et al. (2020) reduce carbon dioxide emissions by providing electricity for buildings and hydrogen for public transport through solar energy. The HRES-H_2 system uses solar PV cells to power the university campus building, and converts the surplus power into hydrogen through the proton exchange membrane electrolyser, which is then used to power the trams in Valgara, Algeria. Assaf et al. (2018) used the multi-objective optimisation of the genetic algorithm to calculate the size of the main equipment of the solar hydrogen coupling system. The goal is to maximise the overall reliability of the system, minimise the energy cost, and minimise the percentage of unused excess energy in PV power generation. Bornapour et al. (2017) established a microgrid model composed of a proton exchange membrane fuel cell combined heat and power, wind turbine, and PV units, and determined the optimal scheduling state of these units by considering the

uncertainty of renewable energy. Guinot et al. (2015) studied the operation of a PV cell system with independent application. The optimal system configuration is determined by optimising the size of components and the parameters of power management strategy, and the power consumption of auxiliary equipment and the aging of components (battery, electrolyser, and fuel cell) is considered. The purpose of the study by Akhtari, Shayegh, and Karimi (2020) was to analyse the hybrid renewable energy system including wind energy, hydrogen energy, and solar energy, to improve the efficiency and reliability of the system, and provide users with power and heat demand. Luta and Raji (2018) made a comparative analysis on the power grid expansion and the implementation of the renewable off-grid hybrid power system. The purpose of the study was to determine the best feasible scheme. Ghenai, Salameh, and Merabet (2020) designed an off-grid solar PV fuel cell hybrid power generation system. The main objective is to optimise the design and development dispatching control strategy of the independent hybrid renewable power system to meet the power load of residential quarters in desert areas. Jahangiri et al. (2019) modelled and quantified the actual electricity production and cost-effective hydrogen based storage systems in several cities in Chad. Xu et al. (2020) proposed a two-stage data-driven multi-criteria decision-making framework to study the optimal configuration of an off-grid wind–light–hydrogen system. In the first stage, a set of Pareto solutions is determined based on the improved non-dominated sorting genetic algorithm. The objective is to simultaneously minimise the average cost of energy, the possibility of power supply loss and the rate of power abandonment. In the second stage, the weights of the three objectives are determined by the importance cross-correlation method, and the unique optimal solution is selected from the Pareto solutions by the similarity ranking technique of ideal solutions. Mehrjerdi (2020) conducted modelling and research on peer-to-peer energy management in buildings. The optimal power of the solar system, power line, fuel cell, and electrolyser, the optimal capacity of the hydrogen storage tank, and the optimal operation mode (charge-discharge mode) of the hydrogen storage system is obtained. Ruiming (2019) proposed an integrated energy system composed of wind turbines, photovoltaic cells, electrolytic hydrogen, fuel cells and hydrogen storage units, and discussed the construction of multi-objective day power dispatching of integrated energy system considering operation and environmental costs. Xu et al. (2018) proposed a multi-objective optimisation model for the configuration of wind power and/or energy storage and/or a local user hybrid energy storage system. A wind farm in Hebei Province is studied and discussed. Through scenario analysis, sensitivity analysis, and comparative analysis, the advantages of the model are demonstrated. Zhang et al. (2020) used a branch cutting algorithm to obtain the minimum annual total cost of the system satisfying different combinations of power load and thermal load: photovoltaic–thermal load–battery, photovoltaic–thermal load–hydrogen, and photovoltaic–thermal load–battery–hydrogen. The influence of heat load on the comprehensive energy efficiency of fuel cell cogeneration is considered. Kikuchi et al. (2018) conducted technical and economic analysis on hydrogen production from photovoltaic power generation using a battery assisted electrolyser. The installed capacity of each module technology is optimised for various unit costs of photovoltaic, battery, and proton exchange membrane electrolyser.

Loisel et al. (2015) evaluated the economics of a hybrid power plant consisting of offshore wind farms and hydrogen production storage systems in the Loire River region of France. Sultan et al. (2020) studied the optimisation design of hybrid renewable energy systems dependent on the power grid and off-grid. The system consists of PV cells, a wind turbine, and a fuel cell with hydrogen tanks to store energy in the chemical form. A new meta-heuristic optimisation technique is used to achieve the optimal component size of the proposed hybrid power system. Zhang et al. (2019) proposed a new hybrid optimisation algorithm for the optimal sizing of a stand-alone hybrid solar and wind energy system based on three algorithms: chaotic search, harmony search, and simulated annealing. Diab et al. (2019) proposed a simulation model to describe the operation of a PV–wind–diesel hybrid microgrid system. Optimal sizing of the proposed system has been presented to minimise the cost of energy supplied by the system while increasing the reliability and efficiency of the system presented by the loss of power supply probability.

As for the CCHP system, many scholars combine solar energy and a CCHP system to add energy storage system, apply new operation strategy, and use a double-layer optimisation algorithm to study. Romero Rodríguez et al. (2016) combined solar energy with a cogeneration system to analyse the configuration of natural gas internal combustion engine, photovoltaic and other equipment, and made a detailed analysis of life cycle cost, emissions, and primary energy consumption. Yang and Zhai (2018) established a mathematical model of the CCHP system mixed with photovoltaic panels and solar collectors. A particle swarm optimisation algorithm is used to find the optimal value of design parameters. Five operation strategies are used in the hybrid system, and the performance of the hybrid system under different operation strategies is analysed. The hybrid system is compared with the conventional system. Yang and Zhai (2019) modelled the CCHP system with a PV system and solar system, and applied the particle swarm optimisation algorithm to find the optimal value of design parameters. Besides, the solar hybrid CCHP systems of three different buildings in seven climate regions of the United States were simulated. Based on the simulation results, the energy output characteristics and operation performance of the solar hybrid CCHP system were studied. Zheng et al. (2019) proposed a new heat storage strategy for the CCHP system, which determines the operation state of a power generation unit according to the power demand, heat demand, and the state of the heat storage device. The working principle of heat storage strategy is introduced and compared with traditional strategy. Taking a hospital in Shanghai as an example, the system performance under different storage strategies is evaluated and compared. Xi et al. (2018) proposed a two-layer optimisation method to optimise the combination of desalination and an independent CCHP system, which is assumed to be installed on a remote South China Sea island. The universal method and branch and bound method are used to solve mixed-integer linear programming optimisation problems in design and operation stages, respectively. Yang et al. (2017) proposed a CCHP and solar thermal coupled compressed air energy storage (S-CAES) system based on the gas turbine. The off-design model of the gas turbine based on CCHP and S-CAES is established. The advantages and disadvantages of two different control strategies are analysed. Ebrahimi and Keshavarz (2015) studied the optimal orientation and size of the solar collector

integrated with the basic CCHP system. The optimum conditions of the solar collector are determined under five different climatic conditions, and the advantages of using the hybrid CCHP system instead of the basic CCHP system are discussed. Wang et al. (2018) proposed a CCHP system combining solar energy and compressed air energy storage. Solar energy and cool storage air conditioning system are combined to heat the high-pressure air in the gas storage. From the perspective of investment cost and efficiency, the multi-objective optimisation method based on a non-dominated sorting genetic algorithm is adopted to obtain the optimal performance of the CCHP system. Ren, Wei, and Zhai (2020) proposed a hybrid CCHP system, and two different solar energy utilising systems are evaluated. The NSGA-II algorithm is used to search for the Pareto front solution of the multi-objective optimisation model considering economic, energy and environmental performance. Li et al. (2020) proposed an improvement strategy following balanced heat-electrical load (FBL) for the CCHP system with a heat pump. The proposed FBL strategy is applied to the CCHP system of a high-speed railway station, and the performance of the FBL strategy is compared with that of the following hybrid electric-heating load (FHL) strategy. Ren et al. (2019) optimised the integrated performance of a hybrid combined cooling, heating, and power system driven by natural gas as well as solar and geothermal energy resources from the energy, economy, and emission perspectives. Li et al. (2019) proposed a combined cooling, heating, and ground source heat pump system with a heat exchanger to improve the comprehensive performance, and compared it with a CCHP–GSHP system without a heat exchanger.

In this chapter, the solar energy, hydrogen production systems, and CCHP systems are combined to realise the system cold–heat–electricity–hydrogen combined power supply. Taking the total system cost as the objective function, the configuration of the system with the lowest unit energy supply cost is obtained. The optimal system is analysed and described in detail. A reference system was introduced to compare the total cost of the system, primary energy consumption and carbon dioxide emissions. The novelty of this study is that it solves the problem of high light dissipation in China, reduces the survival pressure for traditional enterprises, and reduces a large amount of carbon dioxide emissions. Connecting the building energy system to the public transportation sector by producing hydrogen, providing it to hydrogen-filling stations for hydrogen fuel cell vehicles, to increase the share of renewable energy, and make it feasible from a technical, economic, and environmental perspective.

1.3. Project Overview

Energy conservation, emissions reduction, and environmental protection are China's basic state policies. The Outline of the 12th Five-Year Plan for National Economic and Social Development sets clear targets: ‘By 2020, the Chinese government promises that non-fossil energy will account for about 15% of primary energy consumption, and the carbon dioxide emissions per unit of GDP will be reduced by 40 to 45% compared with 2005 levels’. On 10 September 2013, the State Council issued the notice of the State Council on the action plan for the prevention and control of air pollution. In the document, clear requirements are put forward for the concentrations of inhalable particulate matter and

fine particulate matter (PM) reduction index in the Beijing Tianjin Hebei region, Yangtze River Delta, and Pearl River Delta to the end of 2017. By 2017, the PM10 concentration in regional and the abovementioned cities in China will be reduced by more than 10% compared with 2012. The concentrations of fine particles in the Beijing Tianjin Hebei region, the Yangtze River Delta region, and the Pearl River Delta region decreased by 25%, 20%, and 15%, respectively. The average annual concentration of fine particles in Beijing is about 60 microgram per cubic metre of air ($\mu g/m^3$).

In order to implement the notice of the State Council on printing and distributing the action plan for the prevention and control of air pollution, the government has strengthened the prevention and control of air pollution and the improvement of air quality in Beijing, Tianjin, and Hebei and the surrounding areas. In addition, according to the requirements of the State Council, the Ministry of Environmental Protection and the State Energy Administration issued a guide for the implementation of the action plan for the prevention and control of air pollution in Beijing, Tianjin, Hebei, and surrounding areas.

In recent years, the national economy of Panjin City has achieved rapid development. Its comprehensive strength has been significantly enhanced, the urban and rural outlook has been continuously improved, and people's living standards have been significantly improved. The Panjin municipal government actively implements the macro-control policies of the central government, closely combines the actual situation of Panjin City, and strives to speed up the development in the adjustment and take the lead in the competition. A series of strong measures have been taken actively, scientifically, and decisively to maintain the steady and healthy economic development of Panjin City, and to increase the income of urban and rural residents year by year.

From the existing problems in the national economic and social development of Panjin City, it can be seen that the contradiction between environmental capacity, energy resource carrying capacity, and accelerating development is sharp, the rigid constraint of energy resources and environment on economic development is prominent, and the need to adjust the industrial structure and transform the mode of economic development is urgent. Therefore, we should follow the development path of ‘scientific development, green rise’, develop renewable energy, cultivate and strengthen related industries, form new economic growth points, and promote the transformation of economic development mode from resource-dependent to multi-support At present, the utilization of solar energy resources is one of the important development directions of national energy strategy. The rational development of solar energy resources in Panjin City can promote the development of related industries and provide strong support for Panjin Economic Development.

Solar energy is a renewable, clean source of energy. Solar power is the process of converting local natural solar energy into electricity. The production process does not emit any harmful gas and does not pollute the environment. The Law on the Prevention and Control of Air Pollution of the People's Republic of China sets clear limits on pollutant emission standards or total volume control targets for newly built or expanded thermal power plants that emit sulphur dioxide. With the gradual increase of the enforcement of

this law, the investment cost of the new thermal power plant, and the cost of the technical transformation of the existing thermal power plant will increase greatly. In this case, the use of solar energy to generate power will be no fuel consumption and no 'three wastes' emissions. The solar power station will implement greening projects at the same time, these play a role in promoting the development of the local vegetation and trees, protecting land resources, adjusting the ecological environment, as well as improving the regional climate environment.

Panjin area is rich in solar energy resources in Liaoning Province. The development and construction of the Gada Lou Reservoir PV project have a good demonstration role for the construction of photovoltaic power station projects in the region. The construction of the reservoir PV project not only has good economic benefits, but also has significant social benefits. The planned PV power station is located in Dawa, Panjin City, Liaoning Province, and the planning level year is 2021.

Panjin City is a prefecture-level city under the jurisdiction of Liaoning Province. It is located in the central area of the Liaohe River Delta and on the estuary of the Liaohe River. Topographic features are higher in the north and lower in the south, and gradually incline from north to south. Panjin is located in the north temperate zone, it has a warm temperate continental subhumid monsoon climate. The main characteristic of the climate is four distinct seasons. Wind and rain are less in spring. The climate is dry. Liaoning Province has jurisdiction over one county and three districts. The total area is 4,102.9 square kilometres.

2. Research

2.1. Building Description and Climate Description

According to the climate of Panjin, the whole year is divided into three parts: winter (November–February), transition season (March–June, October), and summer (June–September). Three typical days are selected from the three parts, and each typical day is divided into 24 periods. Regional buildings are selected to simulate the change of cooling and heating load, including hotels, office buildings, and shopping malls. The building area of each type is 50,000m^2. The hourly variation of cooling, heating, and power load of each typical day is shown in Figure 4.3. The power demand of the three typical days is relatively stable, the demand for cooling and electricity is dominant in summer, and the demand for heating and electricity is dominant in winter. The data source is from Hua Dianyuan software.

Figure 4.1: Typical Daily Cooling, Heating, and Power Load

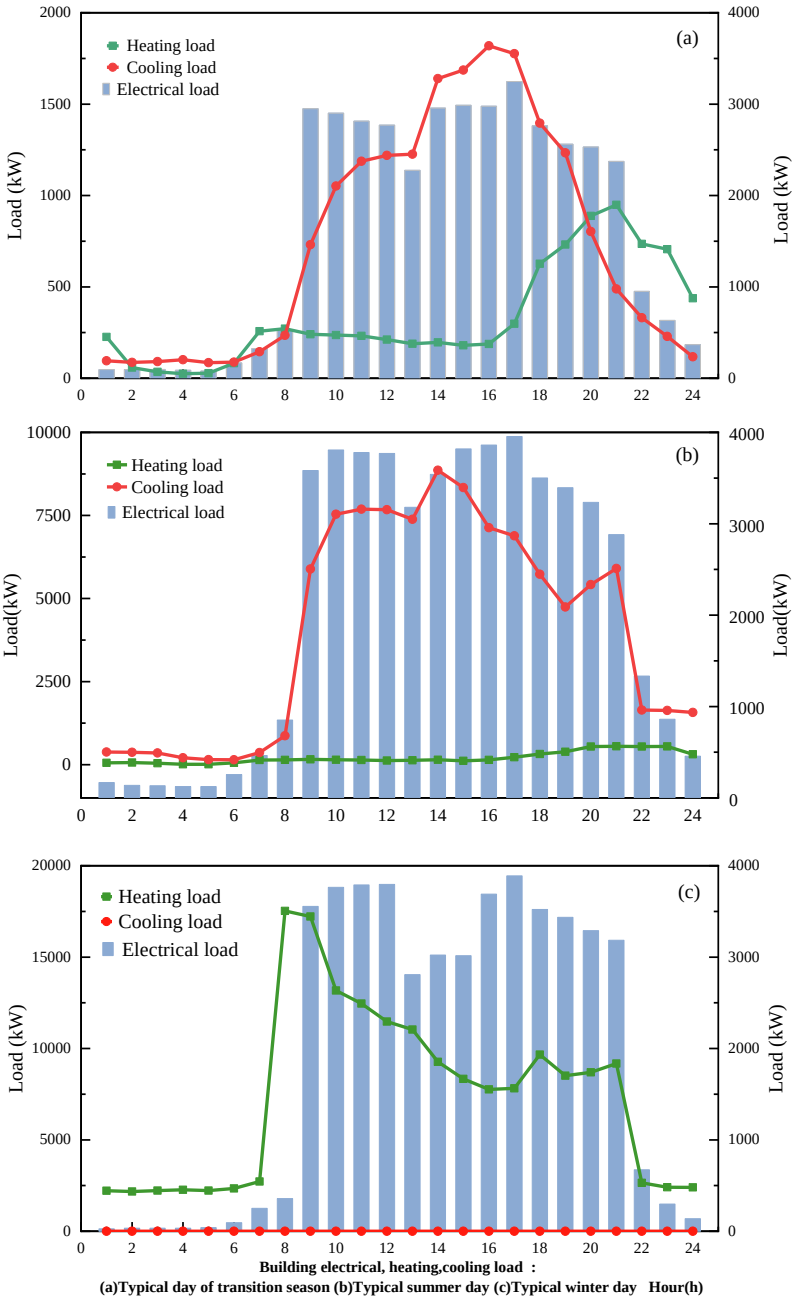

kW = kilowatt.

Source: Hua Dianyuan software.

Figure 4.2: Annual Hourly Solar Radiation in Panjin

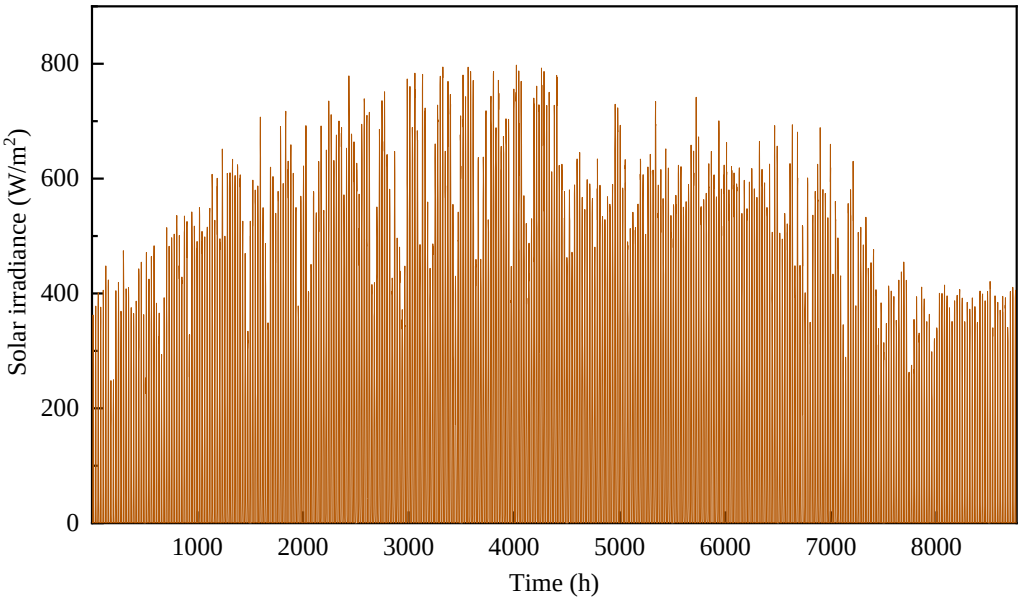

W/m² = watts per square metre.
Source: Hua Dianyuan software.

Figure 4.3: Dry Bulb Temperature and Wet Bulb Temperature

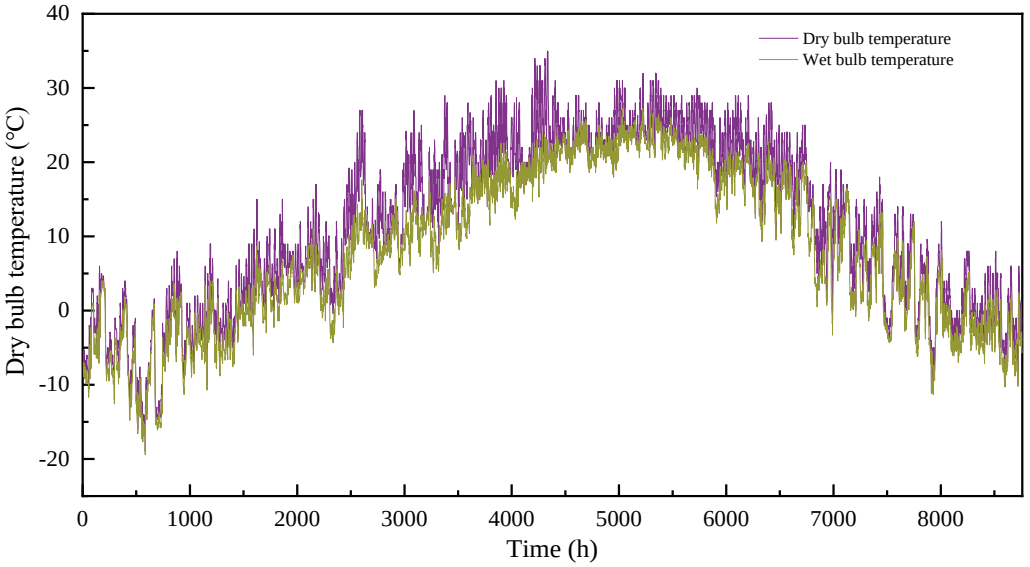

Source: Hua Dianyuan software.

Annual hourly solar radiation in Panjin is shown in Figure 4.2. Dry bulb temperature and wet bulb temperature are shown in Figure 4.3. The average monthly light intensity in Dalian is shown in Figure 4.4a. The light intensity is very high from April to August. It can be seen that the solar radiation intensity reaches the maximum in June and the minimum

in December. The average temperature over 12 months is shown in Figure 4.4b. The temperature is above 20°C from June to September, with the highest monthly average temperature of 25.29°C in August, and below zero in January, February, and December. The lowest temperature is –5.61°C in January.

Figure 4.4. Monthly Average Light Intensity in Dalian

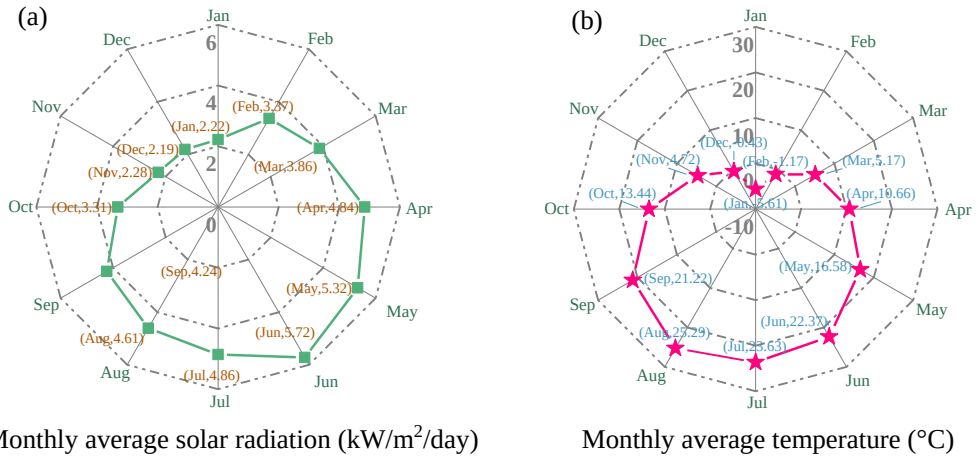

Monthly average solar radiation (kW/m^2/day)

Monthly average temperature (°C)

kW/m^2 = kilowatts per square metre.
Source: Hua Dianyuan software.

2.2. System Description

Dalian is rich in renewable energy, but wind energy is not suitable for large-scale use in urban areas. In contrast, PV panels have broad development prospects in urban high-rise buildings due to their flexible and reliable layout and other natural and technical advantages. Therefore, in this study, a hybrid energy system driven by solar energy and natural gas is proposed and modelled and optimised. The system structure is shown in Figure 4.5. The main demands of buildings include power, hydrogen, heating, and refrigeration. The main power generation equipment in the system are gas turbines and PV cells. When the power of the system cannot meet the load demand of users, the grid supplies power to users. When the light intensity is zero, the system does not produce hydrogen. The generated hydrogen passes through a nearby hydrogenation station to charge the hydrogen fuel cell buses to meet the hydrogen demand. Fuel cell vehicles can be recharged from 9 p.m. to 5 a.m., and the amount of hydrogen required for each fuel cell vehicle is 25 kg/day. This can effectively solve the problem of abandoned light. Absorption chillers and compression chillers provide cooling loads for users, and heat collectors and waste heat recovery systems provide heat energy for users. When the generated heat cannot meet the load demand of users, the auxiliary boiler supplies heat energy to users.

Figure 4.5: CCHP System Flow Chart

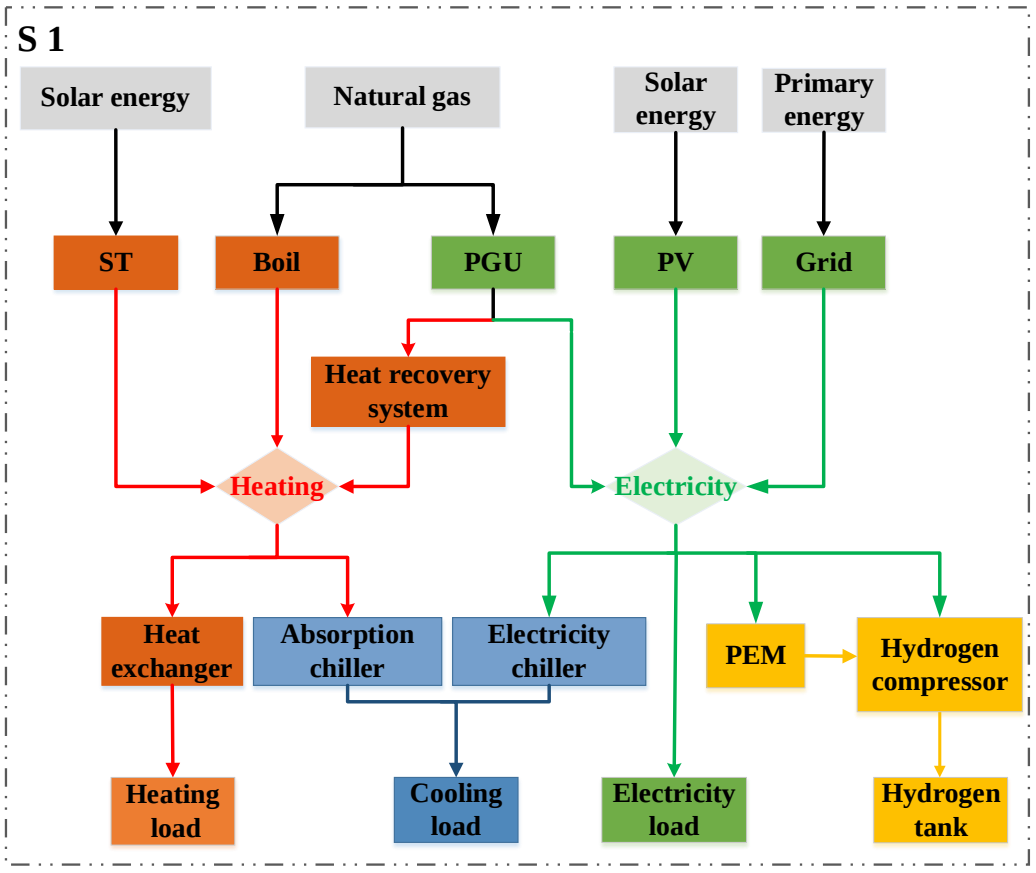

CCHP = combined cooling, heating, and power, PEM = proton exchange membrane, PGU = power generation unit, PV = photovoltaic, S = System 1, ST = solar thermal collector.
Source: Prepared by author.

Figure 4.6: System Diagram

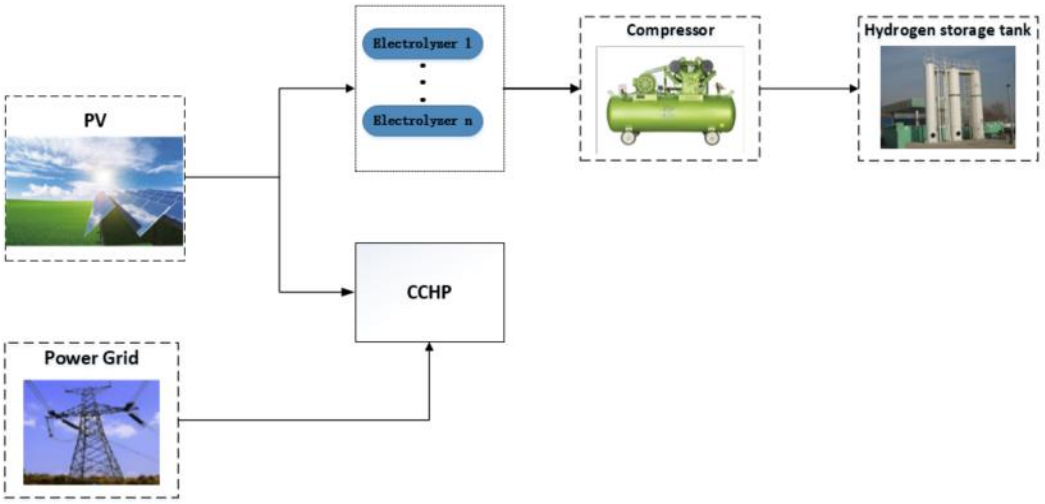

CCHP = combined cooling, heating, and power, PV = photovoltaic.
Source: Prepared by author.

The equipment parameters of the system and their costs are shown in Table 4.1 and Table 4.2.

Table 4.1. Equipment Costs of the System

Facility	Unit	Price
Absorption chiller	$/kW	216
Electricity chiller	$/kW	134
Boiler	$/kW	25
Heat exchanger	$/kW	22
Power generation unit	$/kW	584
PEM	$/kW	353
Hydrogen tank	$/kg	400
Compressor	$/kW	83
PV	$/kW	250
Solar thermal collector	$/kW	200

kW = kilowatt, PEM = proton exchange membrane, PV = photovoltaic,
Sources: Obara and Li (2020); Ma, Fang, and Liu (2017).

Table 4.2: Equipment Parameters of the System

Parameter	Symbol	Value
Gas turbine efficiency	$\eta_{pgu,e}$	35%
Coefficient of performance of electricity chiller	COP_{ec}	3.00
Efficiency of the heat recovery system	η_{rec}	80%
Heat exchanger efficiency	η_{he}	80%
Coefficient of performance of absorption Chiller	COP_{ac}	0.7
Gas-fired boiler	η_b	79%
Generation efficiency of the power grid	η_e	35%
Transmission efficiency of the power grid	η_{grid}	92.2%
Efficiency of solar collector	η_{ST}	75%
Solar photovoltaic efficiency	η_{PV}	16%
PEM efficiency0	η_{el}	90%

PEM = proton exchange membrane.
Source: Akhtari, Shayegh, and Karimi (2020).

Photovoltaic

Extensive solar power generation is the current mainstream of a form of new energy power generation, but also the world's key planning of the development of content. This power generation method is mainly based on the principle of PV effect to directly convert ground solar energy into electric energy. The whole process is noise-free and pollution-free, and is not limited to regional distribution, with small volumes and a long service life. It is a new energy power generation form vigorously promoted by countries around the world. In the process of power generation, the photovoltaic array panel is the basis of the system and the core of energy conversion. In practical application, in order to improve the capacity of the PV array, multiple PV cells are connected in series to form the corresponding square array, which is convenient for the expansion and specification design of the system. In this chapter, the area of each PV plate is 1.6m^2, and the total area of the PV system is expressed by Eq.1.

$$A_{PV} = 1.6 N_{PV} \tag{1}$$

The total output of the PV array is expressed by Eq.2 **Error! Reference source not found.**.

$$P_{PV}(t) = A_{PV} \eta_{PV}(t) G(t) \tag{2}$$

where η_{PV} is the efficiency of PV panel, $G(t)$ is the solar radiation intensity in kW/m^2/h.

Proton exchange membrane

The traditional electrolytic cell operates with a constant hydrogen production rate under the condition of stable electric energy, while the wind power and PV in the integrated energy power generation system are intermittent and random, so the electrolytic cell should be able to produce hydrogen safely and reliably under the condition of unstable electric energy. At present, basic electrolytic cells and proton exchange membrane electrolysers are widely used in integrated energy power generation systems in the world, because these two kinds of electrolysers can operate stably under intermittent fluctuating power, high pressure, high current density and low voltage.

The working principle of the electrolyser is to electrolyse water to produce hydrogen and oxygen. The hydrogen produced is stored in a hydrogen storage tank for sale.

The mass flow rate of hydrogen generated per second (kg/s) is calculated by Eq.3 0.

$$\dot{m}_{H_2} = \frac{E_{el} \times \eta_{el}}{LHV} \tag{3}$$

The amount of hydrogen produced per hour (kg/h) in the mathematical model is shown in Eq.4 0.

$$\Delta H = \frac{E_{el} \times \eta_{el} \times 3600}{LHV} \tag{4}$$

where, LHV is the calorific value of hydrogen, 143 MJ/kg 0.

Power generation unit

The gas turbine is widely used in the microgrid because of its small size, long life, high reliability and low environmental pollution. By burning natural gas, the micro gas turbine drives the generator to provide power loads for the system. At the same time, the waste gas with a large amount of heat generated by the micro gas turbine can be recycled by the waste heat recovery system of the CCHP system, which can directly provide the heating load demand for the system, and can also provide the cooling load demand for the system through the absorption refrigeration mechanism. The power generation efficiency of the gas turbine varies with the change of equipment load rate. Low load rate f will lead to a decrease in equipment efficiency. To avoid the prime mover running with too low efficiency, the switching coefficient of the equipment is set, α = 25%(as the Eq. 5)

$$E_{pgu} = \begin{cases} 0 & 0 \le f < 25\% \\ F_{pgu} \times \eta_{pgu,\mathrm{e}} & 25\% \le f < 100\% \\ P_{pgu} & f \ge 100\% \end{cases} \tag{5}$$

Power grid

When the power generated by photovoltaic and prime mover is not enough to meet the power consumption of users, insufficient power is provided by the grid. The power of the grid is shown in Eq. 6.

$$E_{grid} = F_e \times \eta_e \times \eta_{grid} \tag{6}$$

where η_e is the generation efficiency of the grid, η_{grid} is the transmission efficiency of the power grid.

Heat recovery system

The temperature of waste heat flue gas produced by the gas turbine is as high as 450–550°C, which can be recycled by the waste heat recovery system. After the waste heat generated by the gas turbine is recovered by the waste heat recovery device, it can be used step by step. The heat recovered from the waste heat recovery system is shown in Eq. 7.

$$Q_{rec} = F_{pgu} \times \left(1 - \eta_{pgu,e}\right) \times \eta_{rec} \tag{7}$$

where η_{rec} is the efficiency of the heat recovery system.

Boiler

The gas boiler is different from the micro gas turbine to generate electric energy after burning natural gas, but after burning natural gas to generate high temperature steam, to provide users with hot load and cold load requirements. When the heat generated by a board and waste heat recovery device cannot meet the cold and hot demand of users, the gas boiler will supplement the insufficient heat, as Eq.8 shows.

$$Q_b = F_b \times \eta_b \quad (8)$$

Heat exchanger

The heat is provided to the user through the heat exchanger, and the efficiency relationship of the heat exchanger as Eq.9 shows.

$$Q_h = Q_{he} \times \eta_{he} \quad (9)$$

Absorption chiller

In the hybrid energy system, an absorption chiller is introduced into the system to provide cooling loads for the system by using the high temperature exhaust gas produced by various power generation equipment. It can not only improve the comprehensive energy utilisation efficiency of the system but also effectively improve the operation mode of the system. At present, waste heat drive technology mainly includes absorption refrigeration technology and adsorption refrigeration technology, amongst which absorption refrigeration technology has been widely used in practice. At present, the most widely used absorption chillers are mainly based on ammonia or lithium bromide. By using the evaporation characteristics of the refrigerant and the absorption and heat dissipation characteristics of the absorbent, the waste heat in the exhaust gas is converted into the cooling load required by the system. Due to the large volume, high cost and corrosive ammonia water, ammonia-water absorption chiller is gradually replaced by lithium bromide absorption chiller with low cost, simple equipment and high reliability, as shown in Eq.10.

$$Q_{ac} = Q_{acr} \times COP_{ac} \quad (10)$$

where COP_{ac} is the coefficient of performance of the absorption chiller.

Electricity chiller

The electricity chiller drives the compressor to work by consuming electric energy, generating the cooling capacity required by the system and supplying the cooling loads of the system. The system consists of a compressor, condenser, refrigeration heat exchanger, throttling mechanism, and some auxiliary equipment. The electricity chiller compacts the gas through the compressor, releases the heat after condensing in the condenser, and then reduces the pressure and temperature through the throttling mechanism. After that, the gas absorbs the heat from the refrigerant and evaporates into steam, which continues to enter the compressor and so on.

When the cooling capacity produced by the absorption refrigerator is not enough to meet the cooling load of users, the insufficient cooling capacity is supplemented by the compression refrigerator. The compression refrigerator drives the compressor to work through the consumption of electric energy, to generate the cooling capacity required by the system and supply the cooling load of the system. Cooling load from a compression refrigerator is calculated by Eq.11.

$$Q_{ec} = E_{ec} / COP_{ec} \quad (11)$$

where, Q_{ec} is the cooling capacity produced by the compression refrigerator, COP_{ec} is the coefficient of performance of a compression refrigerator, E_{ec} is the power consumption of the compression refrigerator.

Hydrogen compressor

The power consumed by the hydrogen compressor is shown in Eq.12,

$$E = m_{h2} \times n \times \frac{k}{k-1} \times R \times T \times \left[\left(\frac{P_{n+1}}{P_1} \right)^{\frac{k-1}{nk}} - 1 \right] \times \frac{1}{3600} \quad (12)$$

where, the specific heat ratio k =1.4, the gas constant of hydrogen R=4.157 (KJ/kg.K), the inlet gas temperature T=290K, the absolute pressure P_1=1.5MPa, the outlet pressure P_{n+1}=20MPa, the order n=1.

Solar thermal collector

The total output of the ST is shown in Eq.13.

$$Q_{ST}(t) = A_{ST} \eta_{ST}(t) G(t) \quad (13)$$

where, η_{ST} is the efficiency of solar thermal collector, $G(t)$ is the solar radiation intensity in kW/m^2/h.

2.3. Equilibrium Equation

Electric balance

According to the energy balance, the sum of PV power generation, generator power generation, and grid power generation should be equal to the sum of the user's power loads, power consumption of refrigerators, and electrolysers. As shown in Eq.14.

$$E_{pgu} + E_{PV} + E_{grid} = E + E_{ec} + E_{el} + E_{com} \quad (14)$$

Heat balance

The sum of the heat recovery system, the heat of the photovoltaic and the heat of the boiler is equal to the sum of the heat required by the absorption refrigerator and the heat of the heat exchanger, as Eq.15 shows.

$$Q_{pgu,r} + Q_{ST} + Q_b = Q_{acr} + Q_{he} \quad (15)$$

Cold balance

The refrigeration capacity of the absorption refrigerant and compression refrigerator should meet the cooling load required by users. As shown in Eq.16.

$$Q_{ec} + Q_{ac} = Q_c \quad (16)$$

In the optimisation analysis of the hybrid energy system, some important assumptions are as follows.

(a) It is assumed that the hybrid energy system is completely reliable.

(b) The tilt angle of PV is equal to the local dimension.

2.4. Objective Function

In this chapter, the annual cost of the optimal objective function to optimise so it is given as Eq. (17).

$$ATC = C_{ini} + C_{O,M} + C_{fule} \tag{17}$$

where, C_{ini} is the annual capital recovery cost, including equipment costs, engineering costs and some indirect costs. C_{ini} can be obtained from Eq.18. $C_{O,M}$ is the operation and maintenance cost of the system, as shown in Eq.20. C_{fule} is the cost of raw materials consumed by the system, as shown in Eq.21.

$$C_{ini} = \left(\sum_{i=1}^{n} P_{rated,i} \Phi_i \right) \left(1 + f_{other}\right) f_{cr} \tag{18}$$

where, f_{other} is the conversion factor of other costs, including other auxiliary equipment costs, engineering costs and indirect costs. The capital recovery coefficient f_{cr} is shown in Eq.19. Φ_i is the unit cost of the equipment. The value of f_{other} is shown in Table 4.3.

$$f_{cr} = \frac{r\left(1+r\right)^m}{\left(1+r\right)^m - 1} \tag{19}$$

where, the superscript *m* is the lifetime of the system, which is assumed to be 20 years.

$$C_{O,M} = \left(\sum_{i=1}^{n} P_{rated,i} \Phi_i \right) f_{O,M} \tag{20}$$

$$C_{fule} = \sum_{t=1}^{8760} \left(F_{s,t} C_g + E_{grid} C_e \right) \tag{21}$$

The value of $f_{O,M}$ is shown in Table 4.3. The value of C_g and C_e are shown in Table 4.4.

The cost and replacement cost can be calculated by Eq.22–25**Error! Reference source not found.** .

$$C_{ele} = PAF\left(P_{ele} \times C_{ele}\right) \tag{22}$$

$$C_{re,ele} = PAF\left[P_{ele} \times C_{ele} \times FPF\left(10\right)\right] \tag{23}$$

$$FPF\left(k\right) = \left(1+j\right)^{-k} \tag{24}$$

$$PAF = \frac{j(1+j)^n}{(1+j)^n - 1} \quad (25)$$

where PAF represents the factor of converting present value to annual value, *j* and *n* are the annual interest rate and the electrolyser lifetime which in this chapter are assumed as 5% and 10 years, *FPF(k)* denotes the factor of convert final value to present value, where *k*=10.

2.5. Evaluating Indicator

Unit energy cost is used to evaluate the economic feasibility of the system. According to different hydrogen demands, the equipment configuration with the lowest unit energy cost is selected. Unit energy cost ($/kWh) can be calculated by Eq.26.

$$UEC = \frac{ATC}{E_{served} + C_{served} + H_{served} + H_{2served}} \quad (26)$$

Primary energy consumption (*PEC*) is the primary energy consumption of the system, including natural gas consumption and coal consumption of the power grid, as Eq.27 shows. To meet the strategic requirements of national energy utilisation, the lower the consumption of primary energy, the better.

$$PEC = F_{b,tot} + E_{grid,tot} + F_{en,tot} = \sum_{t=1}^{8760}\left(F_{b,tot} + \frac{E_{grid}}{\eta_e \times \eta_{grid}} + F_{en} \right) \quad (27)$$

China's commitment is to reach the peak of carbon dioxide emissions by 2030 and strive to achieve carbon neutrality by 2060. Therefore, carbon dioxide emissions (*CDE*) is an important indicator to measure whether the system is in line with the goal of energy and environmental friendliness, as Eq.28 shows. The value of f_e and f_g is shown in Table 4.3.

$$CDE = F_{b,tot} \times f_g + E_{grid,tot} \times f_e + F_{en,tot} \times f_g \quad (28)$$

Table 4.3: Main Parameters in the Optimisation Calculation

Parameter	Symbol	Value
Proportion factor of other costs	f_{other}	0.5
Proportion coefficient of operation and maintenance	$f_{O,M}$	0.02
Carbon emission coefficient of natural gas	f_g	0.2(kg/kWh)
Carbon emission coefficient of the power grid	f_e	0.977(kg/kWh)

Source: Li (2017), Benefits Evaluation of Building-scale and District-scale Cooling Heating and Power System [D]. Dalian University of Technology.

Table 4.4: Natural Gas and Electricity Prices in Dalian Area

	Electricity			Natural gas
Time	(8:00-11:00) (17:00-22:00)	(0:00-5:00) (22:00-24:00)	(5:00-8:00) (11:00-17:00)	
Unit price ($/kWh)	0.1736	0.08673	0.1158	0.03262

kWh = kilowatt hour.

Source: Li (2017), Benefits Evaluation of Building-scale and District-scale Cooling Heating and Power System [D]. Dalian University of Technology.

2.6. Operation Strategy

The generation capacity of PV cells and the heating capacity of collectors give priority to meet the electricity demand and heat demand of users. When the power consumption is insufficient, generators will supplement the insufficient power. When the heat is insufficient, boilers will supplement the insufficient heat. When there is sufficient PV power, it is used for the electrolysers and the compressors to produce hydrogen and compress hydrogen. When there is no light intensity and PV power is not generated, the electrolysers and the compressors will not operate, as Eq.10 shows. The system produces different kilograms of hydrogen (from 100 kg/day to 1000 kg/day), and the corresponding equipment capacity is different. The optimal hydrogen supply of the system is determined by comparing the unit energy cost, primary energy consumption, carbon dioxide emission and total cost.

$$\begin{cases} E_{pgu} + E_{PV} = E + E_{ec} + E_{el} + E_{com} & E_{PV} > 0 \\ E_{pgu} + E_{grid} = E + E_{ec} & E_{PV} = 0 \end{cases} \tag{29}$$

The main restriction is that the power and heat output of all installed equipment should not exceed the rated power, and the daily hydrogen production should be greater than or equal to the demand, as Eq.30 shows.

$$\begin{aligned} & Q_{i,t} \le Q_{i,rated} \quad \forall i,t \\ & E_{i,t} \le P_{i,rated} \quad \forall i,t \\ & H_2 \ge W \quad W = 100kg/d \square 1000kg/d \end{aligned} \tag{30}$$

3. Results and Discussion

3.1. Comparative Analysis of Operation Results

The hydrogen production of the system varies from 100 kg/day to 1000 kg/day. The total cost, unit energy cost, primary energy consumption, and carbon dioxide emissions of the system are shown in Figure 4.7 and Table 4.5. It can be seen that the total cost of the system increases steadily with the increase of hydrogen production. Carbon dioxide emissions and primary energy consumption have a similar trend because the carbon dioxide emitted by the system is mainly produced by the combustion of primary energy.

Carbon dioxide emissions and primary energy consumption increased rapidly with the increase of hydrogen production before 300 kg/day, and reached the extreme value at 300 kg/day and 600 kg/day, with slight fluctuation between them. Carbon dioxide emissions and primary energy consumption of the system with hydrogen production of 700 kg/day decreased rapidly, and then decreased slowly and tended to be stable. At the same time, the unit energy cost decreases with the increase of hydrogen production, reaches the lowest value at 700 kg/day, and then increases rapidly. When the daily hydrogen production of the system is 700kg, the unit energy cost is the lowest, and the primary energy consumption and carbon dioxide emissions are relatively low. Therefore, the optimal hydrogen production of the system is 700 kg/day.

Figure 4.7: Total Cost, Unit Energy Cost, Primary Energy Consumption, and Carbon Dioxide Emissions of the System

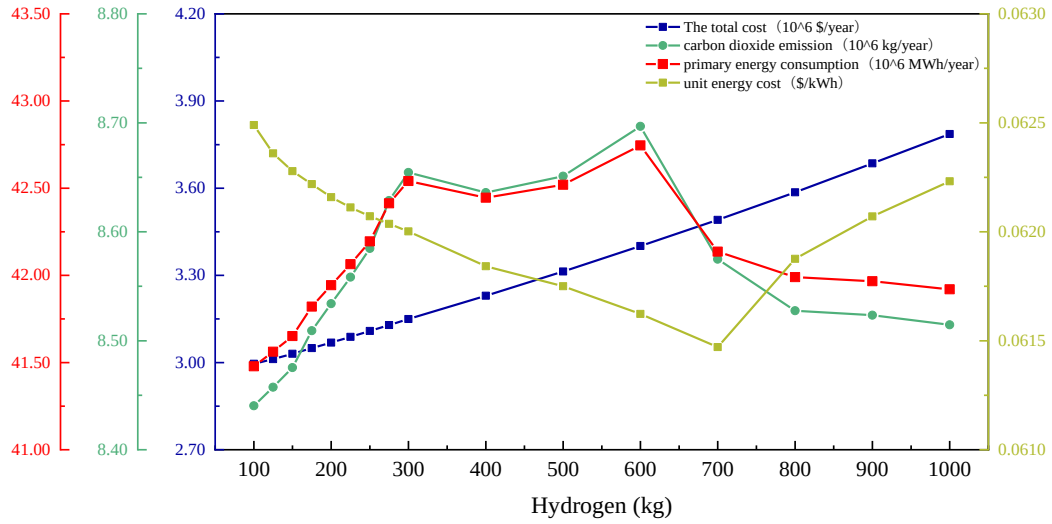

kg = kilogram, kWh = kilowatt hour, MWh = megawatt hour.
Source: Prepared by authors.

The optimal configuration of the system is shown in Table 4.5 when the amount of hydrogen produced by the system is from 100 kg/day to 1000 kg/day.

Table 4.5: Optimal Configuration of the System for Different Hydrogen Production

(The unit of H_2 is kg per day and the rest is kW)

H_2	PV	PEM	ST	PGU	AC	Boil	WHRS	Com
100	5972	514	11008	3640	7655	13615	5,408	21
200	6429	1054	10809	3635	7516	13639	5,400	44
300	7086	1600	10522	3627	7315	13675	5389	66
400	8966	2141	9767	3605	6786	13771	5357	89
500	9462	2692	9912	3600	6888	13767	5348	112

600	10320	3284	9738	3590	6766	13796	5333	136
700	12072	3849	9475	3570	6582	13848	5303	160
800	13160	4528	9329	3557	6480	13879	5285	188
900	14482	5245	9007	3542	6255	13929	5262	217
1000	15804	5962	8712	3527	6048	13977	5240	247

PV = photovoltaic, PEM = proton exchange membrane, ST = solar thermal collector, PGU = power generation unit, AC = absorption chiller, WHRS = waste heat recovery system, Com = hydrogen compressor.
Source: Prepared by authors.

3.2. Comparative Analysis of Reference System

Reference system 1 (Ref 1): the power demand of users is met by the power generation of local thermal power plants and transmitted to the power grid. The cold demand is met by the compression chiller, and the power of the compression chiller is provided by the power grid. The heat demand is met by gas boilers. Hydrogen is produced by coal gasification and transported to hydrogenation stations by storage and road transportation.

Reference system 2 (Ref 2): compared with Ref 1, the supply mode of cooling, heating and power is the same. Hydrogen is provided by the centralised hydrogen production plant of natural gas and transported to the hydrogenation station through storage and transportation and road transportation.

Reference system 3 (Ref 3): it is composed of a CCHP system and centralised hydrogen production mode of the natural gas plant. The electricity demand of users is provided by photovoltaic power generation, internal combustion engine power generation and the power grid. Heat demand is provided by solar collectors, boilers, and heat recovery systems of internal combustion engines. Cold demand is provided by absorption chillers and compression chillers. The mode of hydrogen supply is the same as that of Ref 2.

The cost comparison between the reference system and the design system is shown in Figure 4.8. It can be seen from the figure that the electricity cost, natural gas cost, and equipment cost are the same in the proportion of Ref 1 and Ref 2 costs. Since the cost of centralised hydrogen production from natural gas is higher than that of coal, the total cost of Ref 2 is slightly higher than that of Ref 1. In the total cost of Ref 1 and Ref 2, electricity cost accounts for the largest proportion. In Ref 3 and System 1 (S1), the power cost accounts for a small proportion, because the power demand is mainly provided by internal combustion engine power generation and photovoltaic power generation, and only a small part of the power is supplied by the grid. Overall, the total cost of system S1 is the lowest, in which the equipment cost accounts for a relatively high proportion, followed by the natural gas cost.

Figure 4.8: Cost Comparison Between the Reference System and the Design System

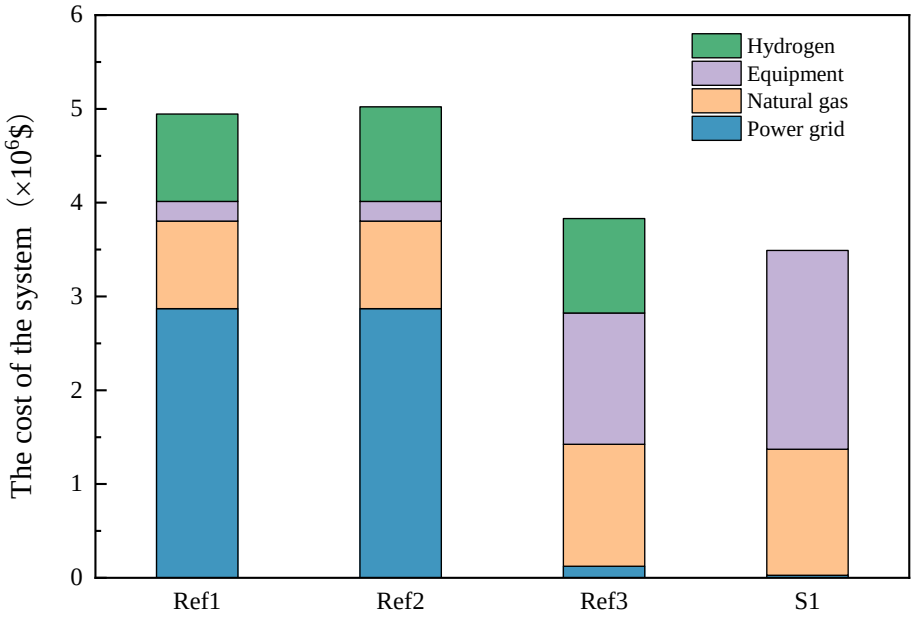

S1= System 1.

Source: Prepared by authors.

The comparison of carbon dioxide emissions between the reference system and the design system is shown in Figure 4.9. As can be seen from Figure 4.9, Ref 1 and Ref 2 have high carbon dioxide emissions. This is because the power of Ref 1 and Ref 2 is provided by the power plant, which will produce a lot of carbon dioxide when generating electricity. Because the hydrogen in Ref 1 is produced from coal, the carbon dioxide emission of Ref 1 is higher than that of Ref 2. Since the electricity of Ref 3 and S1 is provided by the internal combustion engine and PV, PV power generation does not produce carbon dioxide, so the overall carbon dioxide emission of the system is low. Because the hydrogen of the S1 system is produced by electrolyser, and no carbon dioxide is produced in the process, compared with the Ref 3 system, hydrogen is produced by concentrated hydrogen production from natural gas, so the carbon dioxide emission of the S1 system is the lowest.

Figure 4.9: Comparison of Carbon Dioxide Emissions Between the Reference System and the Design System

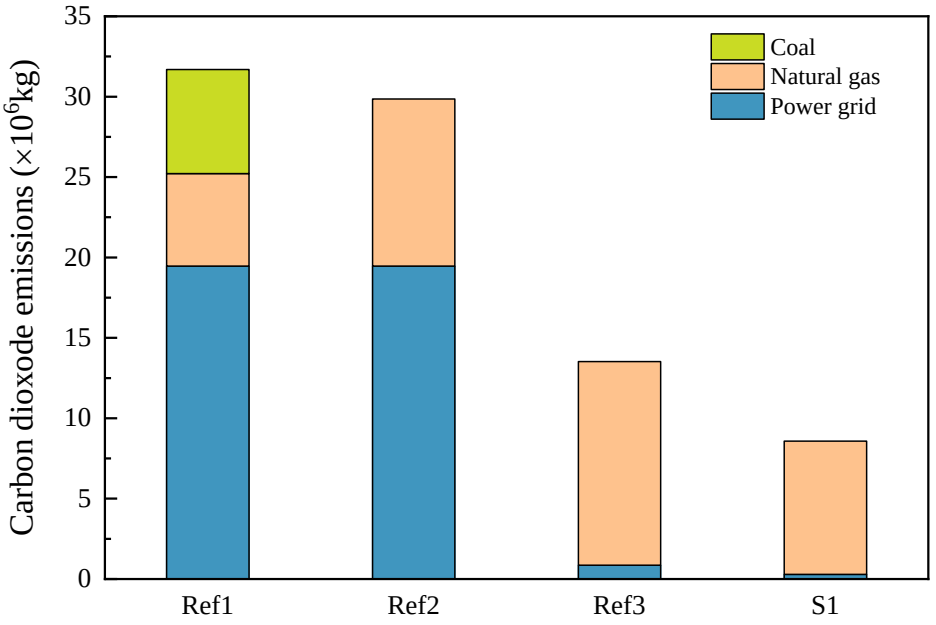

kg = kilogram.
Source: Prepared by authors.

The primary energy consumption of the reference system and the design system is shown in Figure 4.10.

It can be seen from Figure 4.10 that the main primary energy consumption of Ref 1 and Ref 2 is the energy consumption of the power grid. The main primary energy consumption of Ref 3 and Ref 4 is solar energy. Due to the low efficiency of photovoltaic power generation, more solar energy is needed to generate the same power. But solar energy is renewable energy and clean energy, so in general, S1 system energy use is cleaner and more sustainable.

Figure 4.10: Primary Energy Consumption of the Reference System and the Design System

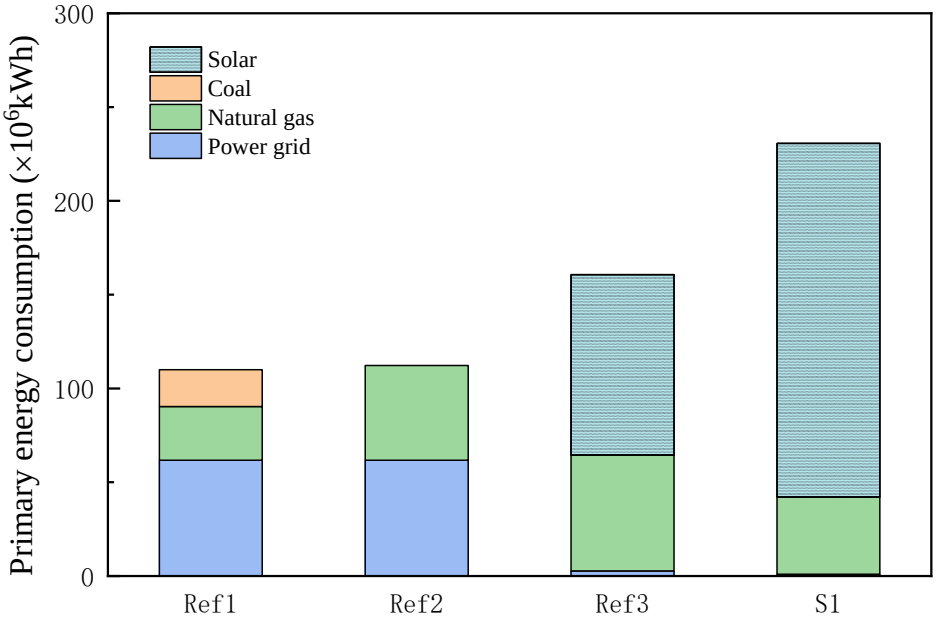

kWh = kilowatt hour.
Source: Prepared by authors.

3.3. Optimal System Analysis

3.3.1. Analysis of Annual Total Energy Supply of the System

As shown in Figure 4.11(a), in the system with daily hydrogen production of 700 kg/day, the hourly power generation curves of the photovoltaic, gas engine, and power grid in 12 typical days are shown. It can be seen that in the typical days of January, February, November, and December, the gas engine has two obvious peaks in a day, just because the light intensity is weak, and the light time is short in winter. In the morning and evening, the PV power generation is not enough to meet the power consumption of the system, and the engine power generation is needed to supplement the insufficient power. When the demand is small, the internal combustion engine will not run when the power is small due to the start-stop constraint, and the insufficient power will be made up by the power grid. In winter and transition season, the power generated by an internal combustion engine is more. In summer, due to the strong light intensity and more photovoltaic power, the power generated by the internal combustion engine is less. Figure 4.11(b) shows the proportion of photovoltaic, internal combustion engine, and power grid in the total power supply of the system in a year. It can be seen that photovoltaic power generation accounts for 76.47%, internal combustion engine power generation accounts for 22.65% of the total power generation, and power grid power generation accounts for only 0.88%.

Figure 4.11: Annual Power Supply of the System

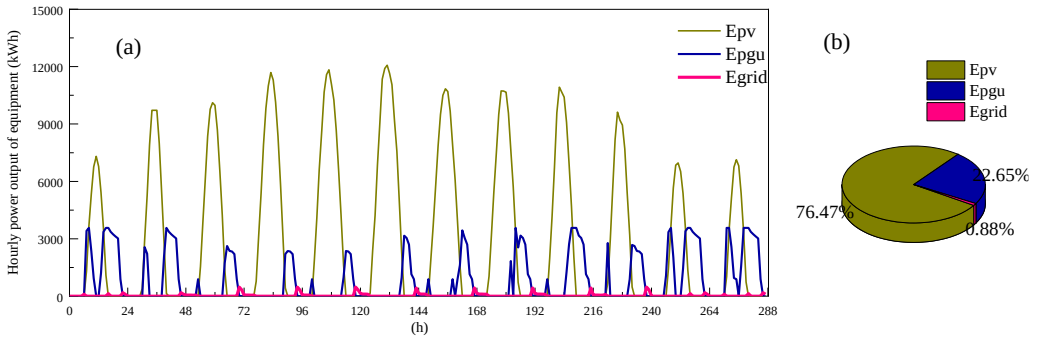

Epv = electricity of photovoltaic, Epgu = electricity of power generation unit, Egrid = electricity of grid, h = hour, kWh= kilowatt hour.
Source: Prepared by authors.

In the system with daily hydrogen production of 700 kg/day, the hourly heating capacity of solar collectors, internal combustion engine waste heat recovery systems, and boilers in 12 typical days is shown in Figure 4.12(a). In January, February, November, and mid-December of winter, the heat output of the boiler is significantly higher than that in other seasons. This is due to the weak light intensity and short light time in winter, and the heat generated by solar collectors is not enough to meet the heat demand of the system, so boilers are used to supplement the insufficient heat. In the typical days of June, July, August, and September in summer, boilers provide heat for the absorption chiller to cool. In the transition season, the demand for heat and cooling capacity is low, so the solar collectors and waste heat recovery systems can meet the needs of users' cooling and heating load, and the calorific value of the boiler is low. As shown in Figure 4.12(b), the annual total calorific value of the solar collectors, waste heat recovery system, and boilers is relatively balanced. The calorific value of solar collectors is the highest, accounting for 43.21% of the total calorific value, followed by boilers, accounting for 32.57% of the total calorific value, and the calorific value of the waste heat recovery system accounts for 24.23% of the total calorific value.

Figure 4.12: Annual Heating Supply of the System

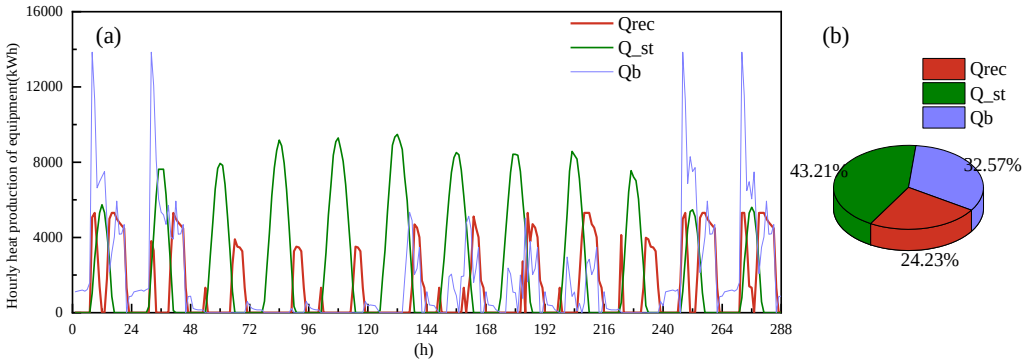

h = hour, kWh = kilowatt hour, Qrec = heat of heat recovery system, Q_st = heat of solar thermal collector, Qb = heat of boiler.

Source: Prepared by authors.

In the system with daily hydrogen production of 700 kg/day, the hourly cooling capacity of the absorption refrigerator and compression refrigerator in 12 typical days is shown in Figure 4.13(a). In winter, there is no cooling load demand, so the cooling capacity of the system is almost zero. As shown in Figure 4.13(b) the cooling capacity provided by the absorption chiller accounts for 89.16% of the total cooling capacity, and the cooling capacity provided by the compression chiller accounts for 10.84% of the total demand.

Figure 4.13. Annual Cooling Supply of the System

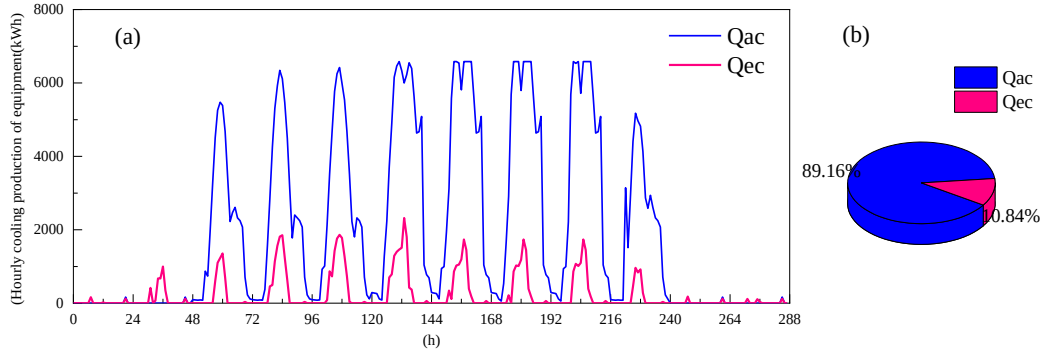

h = hour, kWh = kilowatt hour, Qac = cooling of absorption chiller, Qec = cooling of electricity chiller.

Source: Prepared by authors.

Due to the obvious seasonality, a typical day is selected in winter, summer, and the transition season, respectively for detailed load analysis. Figure 4.14 shows the load balance of cooling, heating, and power in summer.

3.3.2. Cost Analysis

The total cost of the system is composed of capital recovery cost, operation and maintenance cost and fuel cost. As shown in Figure 4.14, the highest proportion of capital recovery cost is 53.96%. Fuel cost accounted for 39.27%, and the lowest operation and maintenance cost was only 6.78%.

Figure 4.14: The Total Cost of the System

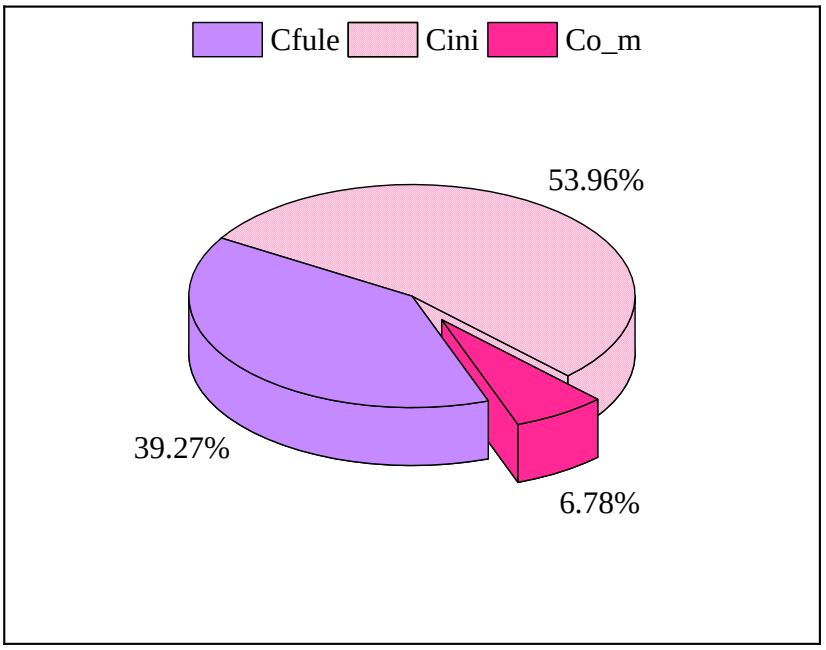

Cfule = fuel cost, Cini = capital recovery cost, Co_m = operation and maintenance cost.
Source: Prepared by authors.

Fuel cost includes the cost of natural gas burned by the internal combustion engine, the cost of natural gas burned by the gas-fired boiler and the cost of buying electricity from the power grid. As shown in Figure 4.15, the cost of natural gas consumed by the internal combustion engine is the most, accounting for 52.03%. The gas-fired boiler also accounts for a large proportion, accounting for 46.04%, while the cost of purchasing electricity in the power grid is only 1.93%.

Figure 4.15: Fuel Cost of the System

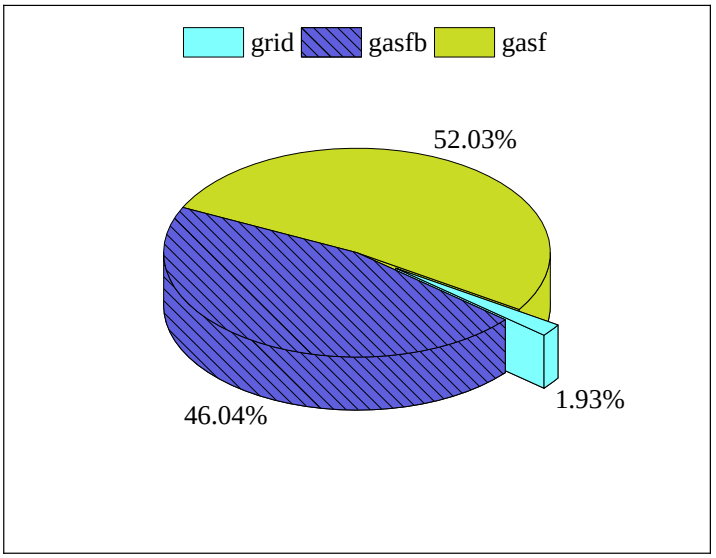

Gasfb = gas fired boiler, gasf = natural gas.
Source: Prepared by authors.

The cost of each piece of equipment in the annual capital cost is shown in Figure 4.16. The cost of photovoltaic is the highest, accounting for 24.48%, the cost of the internal combustion engine is 16.91%, and the cost of solar collector and the electrolytic cell is similar, accounting for 15.37% and 15.08%, respectively. Absorption chillers also account for a large proportion. The cost of heat exchanger, hydrogen storage tank, and boiler accounts for about 2%.

Figure 4.16: Cost of Each Piece of Equipment in the Annual Capital Cost

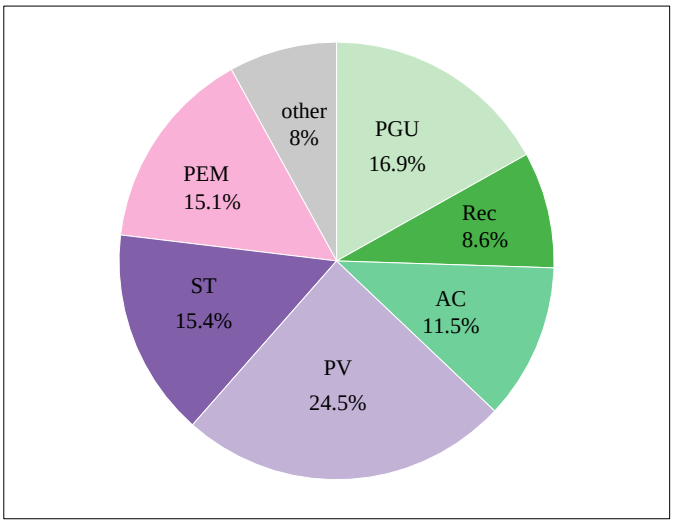

AC = absorption chiller, PEM = proton exchange membrane, PGU = power generation unit, ST = solar thermal collector, Rec = heat recovery system.
Source: Prepared by authors.

3.3.3. Typical Daily Load Analysis

The power output of PV, generator, and the power grid depends on the characteristics of the electric load. The power load, power supply, and hydrogen production of regional public buildings are shown in Figure 4.17(a). The top of the horizontal axis shows the output of the PV, generator, and power grid. The lower part of the horizontal axis indicates the power consumption of the user, the power consumption of the compression refrigerator, the electrolytic cell, and the hydrogen compressor. The black line represents the production of hydrogen at each moment. In summer, the power generation of the system is mainly used for the power load demand of users, followed by the compression chiller and electrolytic cell, and the power consumption of hydrogen compressor accounts for a small part of the total power supply. It can be seen that the amount of hydrogen generated is relatively large from 7:00 to 13:00 on typical days in summer. From 13:00 to 15:00, the power consumption of the compression refrigerator increases greatly, while the user's power consumption still maintains a relatively large demand, which makes the available power of the electrolyser decrease greatly during this period. The hydrogen gas production keeps the same with the change of the power consumption of the electrolyser, and there is no surplus at 15:00 Electricity is used to produce hydrogen for the electrolyser, so the hydrogen production is 0 at this time, and the power consumption of the compressor is also 0. At 16:00 with the decrease of power consumption of the compression refrigerator, the hydrogen production increases again. Then, with the decrease of light intensity, when there is no extra point for hydrogen production, the electrolyser and compressor stop working.

The heat load and heat supply of regional public buildings are mainly provided by solar collectors, heat recovery systems of gas turbines and boilers. As shown in Figure 4.17(b), the heat load and heat supply of a typical day in summer. Above the horizontal axis is the heating capacity of the heating equipment. It can be seen that due to the strong light intensity in summer, the heat supply of solar collectors accounts for a large proportion. The second is the heat recovery system of the gas-fired boiler and internal combustion engine, whose heating period is mainly concentrated in the afternoon when the light intensity is weak and in the evening. Below is the heat required by the absorption refrigerator and the heat exchange of the heat exchanger, that is, the heat load of the user. Since there is a large demand for cooling capacity in summer, we can see that the heat under the horizontal axis is mainly supplied to the absorption chiller for cooling. The heat supplied to the heat exchanger accounts for a small part of the total heat.

The cooling load of regional public buildings is mainly provided by compression chillers and absorption chillers. As shown in Figure 4.17(c), above the horizontal axis is the cooling capacity generated by the compression chiller and absorption chiller, and below the horizontal axis is the cooling capacity required by the regional building. As shown in Figure 4.17, since the solar collector generates a lot of heat, most of the cooling capacity is provided by the absorption chiller. The cooling capacity provided by the compression refrigerator only accounts for 13% of the total cooling capacity.

Figure 4.17. Analysis of Typical Daily Load in Summer

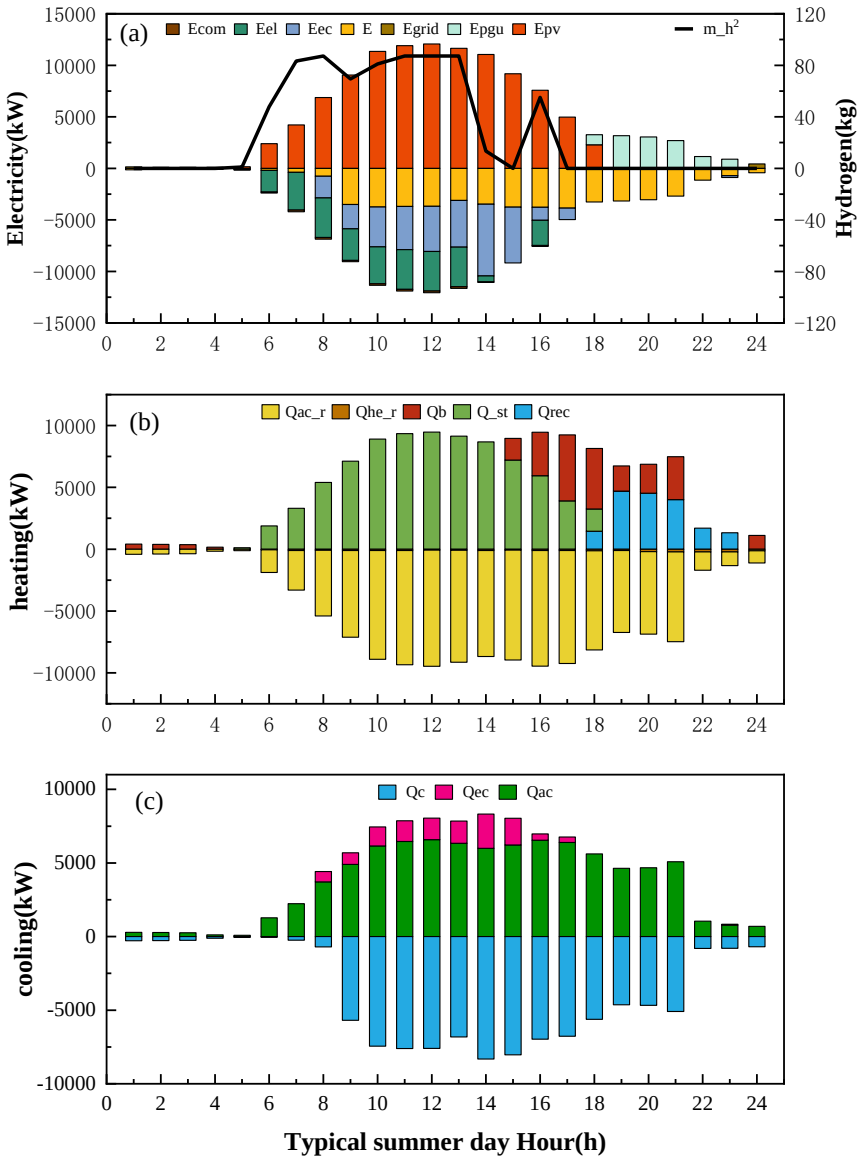

kg = kilogram, kW = kilowatt, Ecom = electricity of compressor, Eel= electricity of electrolyser, Eec = electricity of chiller, E = electrical load, Egrid = electricity of gird, Epgu = electricity of power generation unit, Epv = electricity of photovoltaic, m_h^2 = hydrogen production, Qac_r = heat of absorption chiller, Qhe_r = heat of heat exchanger, Qb = heat of boiler, Q_st = heat of solar thermal collector, Qrec= heat of heat recovery system, Qc = cooling load, Qec = cooling of electricity chiller, Qac = cooling of absorption chiller.
Source: Prepared by authors.

The changing trend of the transition season is similar to that of summer, as shown in Figure 4.18(a). In the transition season, the light intensity is not as high as that in summer, and the corresponding photovoltaic power generation is not as high as that in summer. Therefore, the power generation of the corresponding gas-fired internal combustion engine is increased to meet the demand of the electric load. Due to the low demand for cooling load in the transition season, we can see that the power consumption of the

compression refrigerator is greatly reduced, which is less than that of the electrolytic cell. As shown in Figure 4.18(b), the main heating equipment in the transition season is the solar collector and the heat recovery system, and the boiler only provides a small part of the heat. We can see that the main heat is used in the absorption refrigerator. As shown in Figure 4.18(c), in the transition season, due to the small cooling load, a part of the cooling capacity is wasted.

Figure 4.18: Analysis of Typical Daily Load in the Transition Season

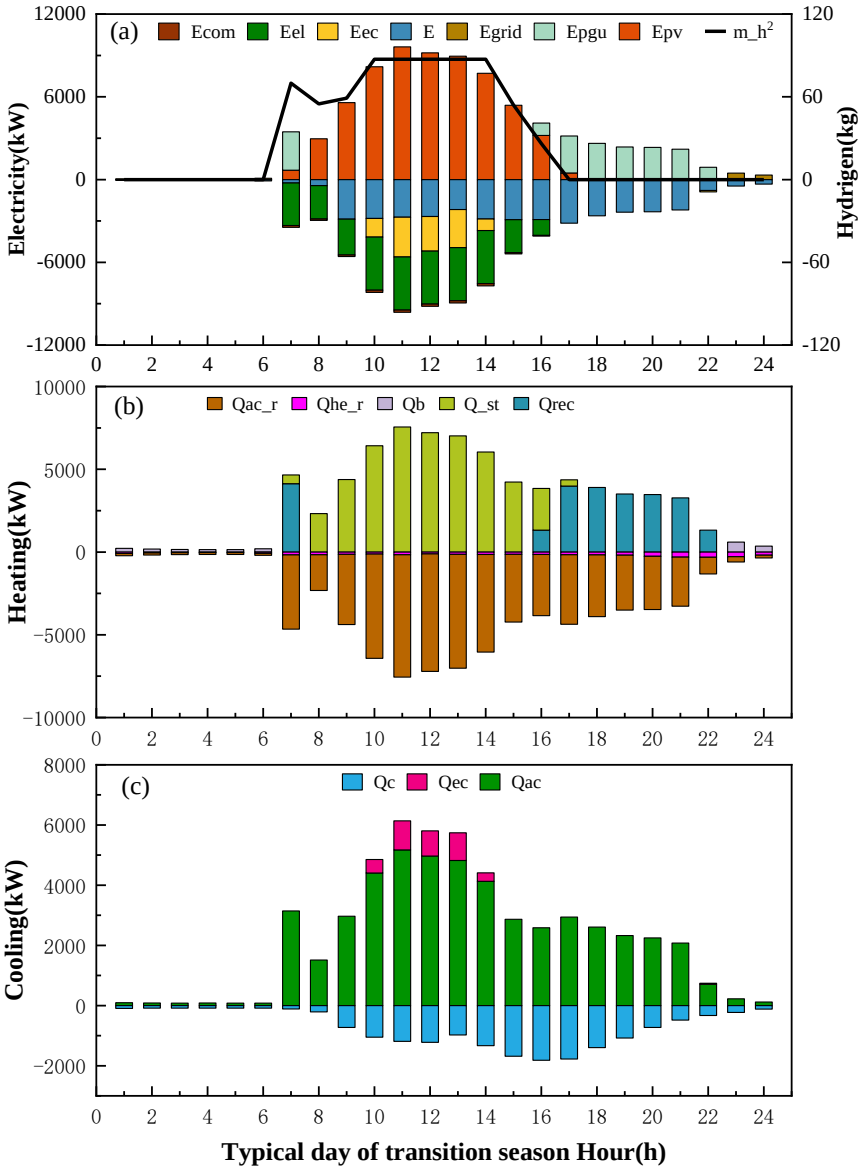

kg = kilogram, kW = kilowatt, Ecom = electricity of compressor, Eel= electricity of electrolyser, Eec = electricity of chiller, E = electrical load, Egrid = electricity of gird, Epgu = electricity of power generation unit, Epv = electricity of photovoltaic, m_h² = hydrogen production, Qac_r = heat of absorption chiller, Qhe_r = heat of heat exchanger, Qb = heat of boiler, Q_st = heat of solar thermal collector, Qrec= heat of heat recovery system, Qc = cooling load, Qec = cooling of electricity chiller, Qac = cooling of absorption chiller.
Source: Prepared by authors.

In winter, as shown in Figure 4.19(a) due to the weakening of light intensity and light time, the photovoltaic power generation is not enough to meet the power load of users. Therefore, it can be seen that when the photovoltaic power is not generated, the gas turbine has been working, and a small part of the power is provided by the grid. At 8 a.m., due to the weak light intensity, the photovoltaic power generation is not enough to meet the power load demand of users, so gas turbine power generation is used to make up for the shortage of electricity, and the excess electricity is used to produce hydrogen. At 9 a.m., with the increase of light intensity, the power of the gas-fired internal combustion engine decreases, and there is no surplus electricity to the electrolytic cell at this time, so the production of hydrogen is 0. In winter, the electric load of users accounts for a large proportion of the total power consumption. The second is the compression refrigerator and electrolyser.

Due to the weak illumination intensity and short illumination time in winter, as shown in Figure 4.19(b), the main heating equipment is the boiler, followed by the heat recovery system of the gas turbine. This is because the cost will be reduced by using the boiler for heating, so when the solar collector does not supply heat, most of the heat is provided by the boiler. Because there is no cold demand in winter, the absorption chiller does not work.

Since there is no cooling load in winter, it is not listed in Figure 4.19.

Figure 4.19: Analysis of Typical Daily Load in Winter

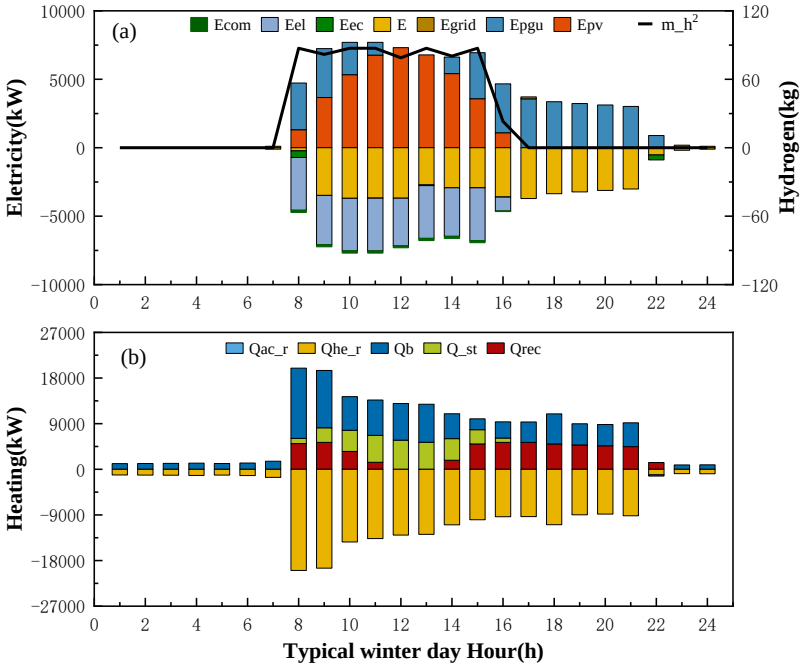

kg = kilogram, kW = kilowatt, Ecom = electricity of compressor, Eel= electricity of electrolyser, Eec = electricity of chiller, E = electrical load, Egrid = electricity of gird, Epgu = electricity of power generation unit, Epv = electricity of photovoltaic, m_h^2 = hydrogen production, Qac_r = heat of absorption chiller, Qhe_r = heat of heat exchanger, Qb = heat of boiler, Q_st = heat of solar thermal collector, Qrec= heat of heat recovery system, Qc = cooling load, Qec = cooling of electricity chiller, Qac = cooling of absorption chiller.
Source: Prepared by authors.

3.3.4. Calculation and Analysis of Hydrogen

The cost of hydrogen mainly comes from three parts: the cost of hydrogen production, the cost of hydrogen compression, and the cost of hydrogen storage. Since the distributed energy system is close to the user, the selected hydrogenation station is very close to the user. Therefore, hydrogen does not need to be transported.

$$CC_{H_2} = C_{H_2} + \mathrm{Cos}\,t_{kgH_{2,com}} + \mathrm{Cos}\,t_{kgH_{2,store}} \tag{31}$$

CC_{H2}—Total cost of hydrogen, \$/kgH_2

C_{H2}—Cost of hydrogen production, \$/kgH_2

$Cost_{kgH2,com}$—Cost of hydrogen compression, \$/kgH_2

$Cost_{kgH2,store}$—Hydrogen storage cost, \$/kgH_2

Cost of hydrogen production

The cost proportion of hydrogen in the system is calculated by Eq.32, and further the cost of hydrogen in the total cost of the system can be solved. The calculation method of hydrogen production cost is as follows:

$$C_{H_2} = \frac{\dfrac{q_{H_2}}{q_{power} + q_{heat} + q_{cool} + q_{H_2}} \cdot ATC}{H_{2,gen}} \tag{32}$$

q_{H2}—Hydrogen calorific value, kWh

q_{power}—Calorific value of electrical load, kWh

q_{heat}—Heating load calorific value, kWh

q_{cool}—Calorific value of cooling load, kWh

The total cost of the system is \$3,491,080.19, the annual total functional capacity 56,792,661.71 kWh, and the annual total hydrogen supply 10,283,337.20 kWh. According to the calculation, the unit hydrogen production cost of the system is \$2.48/kg.

Cost of hydrogen compression

The cost of hydrogen compression is mainly composed of three parts: the cost of the compressor, the cost of electricity consumed by hydrogen compression, and the cost of water consumed by hydrogen compression. The cost of compressor accounts for the highest part. The power needed to compress the gas is provided by the system, which need not be considered here. Hydrogen compressors are designed to compress hydrogen gas, ensuring it is pressurised enough to be stored in hydrogen storage tanks, where it can be transported over long distances and sold throughout the country.

$$\mathrm{Cos\,t}_{kgH_{2,}com} = \frac{H_{2,compower} \times price_{electric} + H_{2,coolwater} \times price_{water} + H_{2,com\cos t}}{H_{2,gen}} \quad (33)$$

$H_{2,compower}$—Power consumption when compressing hydrogen, kWh

$price_{water}$—Water price, $/Lit

$H_{2,coolwater}$—Cooling water volume, Lit

$H_{2,comcost}$—Compressor cost consumption, $

Water cost for compressed hydrogen

$$H_2CoolWater = \frac{H_2ComPower \cdot 50}{2.2} \quad (34)$$

$$H_2ComPower = H_2GenCap \cdot NStages \cdot (\frac{\gamma}{\gamma - 1}) \cdot R \cdot T \cdot (\frac{H_2Com\,\mathrm{Pr}}{Gen\,\mathrm{Pr}})^{(\frac{\gamma-1}{NStages \cdot \gamma} - 1)} \quad (35)$$

$H_2CoolWater$—Water for compressed gas, Lit

γ—Adiabatic index=1.4

R—Gas constant= 4124J/kg.K

T—Temperature=290K

$GenPr$—Hydrogen production pressure

H_2ComPr—Hydrogen storage pressure, MPa

$NStages$—Compressor stage

1.$H_2ComPr<0.5MPa$

2.$0.5MPa<H_2ComPr<5MPa$

3. $H_2ComPr>5MPa$

The calculated compressor cost is $1.34/kg.

The water cost for compressed hydrogen is $0.077/kg.

The total compression cost is $1.417/kg.

Hydrogen storage cost

The cost of hydrogen tank is the main cost in the stage of hydrogen storage.

$$\mathrm{Cost}_{kgH_{2,store}} = \frac{c_{\mathrm{tank}} \cdot p_{\mathrm{tank}} \cdot (n+2) \cdot b}{H_{2,gen}} \qquad (36)$$

c_{tank}—Unit cost of hydrogen storage tanks, \$/kg

p_{tank}—Capacity of hydrogen storage tank, kg

n—Number of hydrogen storage tanks

b—Conversion factor

The cost of hydrogen storage is \$1.93/kg. Therefore, the total cost of hydrogen supply is \$5.827/kg.

Total cost \$/kg	Cost of hydrogen production \$/kg	Cost of hydrogen compression \$/kg	Cost of hydrogen storage \$/kg
5.827	2.48	1.417	1.93

4. Conclusion

To solve the urgent problem of large-scale surplus and demand growth of solar power generation in China, this chapter proposes a solution of CCHP, and analyses the economy, energy, and environment based on the application scenarios. The optimal system configuration for hydrogen supply is selected.

The optimal matching hydrogen load of the system is 700 kg/day, and the unit energy cost of the system is the smallest, which is \$0.0615/kWh. The total cost of the system is \$3,491,080. The annual carbon dioxide emission of the system is 8,574,791 kg, and the primary energy consumption of the system is 4,213,5860 MWh. The capacity of photovoltaic equipment is 12,072 kW, that of the gas turbine is 3,570 kW, and that of an electrolytic cell is 3,849 kW.

In comparison with the reference system, it can be concluded that the total cost, carbon dioxide emissions, and fossil energy consumption of S1 are the lowest amongst the four systems. S1 is more economical and sustainable.

In the system with hydrogen production of 700 kg/day, photovoltaic power generation accounts for 76.47% of the total power generation, internal combustion engine power generation accounts for 22.65% of the total power generation, and power grid power generation accounts for only 0.88%. The calorific value of the solar collector is the highest, accounting for 43.21% of the total calorific value, followed by the boiler, accounting for

32.57% of the total calorific value, and the heat of waste heat recovery system accounts for 24.23% of the total calorific value. The cooling capacity provided by the absorption chiller accounts for 89.16% of the total cooling capacity, and the cooling capacity provided by the compression chiller accounts for 10.84% of the total demand.

In the analysis of typical days, the operation time of the gas engine is short because of the strong illumination intensity and long illumination time in summer. When there is no illumination, the gas turbine will run. In the transition season and winter, especially in winter, due to the weak light intensity and the constraints of daily hydrogen production, the photovoltaic power generation cannot fully meet the power load demand of users, and the internal combustion engine needs to supplement the insufficient power.

In the cost analysis, the capital recovery cost of the system accounts for 53.96%, the fuel cost accounts for 39.27%, and the operation and maintenance cost of equipment accounts for 6.77%. The cost of natural gas in the fuel cost is 98.07% of the fuel cost. In the equipment cost, PV accounted for the highest proportion, which was 24.48%, followed by solar collector and electrolyser, which were 15.37% and 15.08%, respectively.

The part of the system to be improved is that during the transition, most of the cold energy generated by the system is wasted, and further optimisation design is needed to achieve the standard of supply and demand balance.

References

Akhtari, M.R., I. Shayegh, and N. Karimi (2020), 'Techno-economic Assessment and Optimization of a Hybrid Renewable Earth - Air Heat Exchanger Coupled with Electric Boiler, Hydrogen, Wind and PV Configurations', *Renewable Energy*, 148, pp.839–51.

Assaf, J. and B. Shabani, (2018), 'Multi-objective Sizing Optimisation of a Solar-thermal System Integrated with a Solar-hydrogen Combined Heat and Power System, Using Genetic Algorithm', *Energy Conversion & Management*, 164, pp.518–32.

Bornapour, M., R.A. Hooshmand, A. Khodabakhshian, and M. Parastegari (2017), 'Optimal Stochastic Scheduling of CHP-PEMFC, WT, PV Units and Hydrogen Storage in Reconfigurable Micro grids Considering Reliability Enhancement', *Energy Conversion and Management*, 150, pp.725–41.

Diab, A.A.Z., H.M. Sultan, I.S. Mohamed, O.N. Kuznetsov, and T.D. Do (2019), 'Application of Different Optimization Algorithms for Optimal Sizing of PV/Wind/Diesel/Battery Storage Stand-Alone Hybrid Microgrid', *IEEE Access*, 7, pp.119223–45.

Ebrahimi, M. and A. Keshavarz (2015), 'Designing an Optimal Solar Collector (orientation, type and size) for a Hybrid-CCHP System in Different Climates', *Energy & Buildings*, 108, pp.10–22.

Ghenai, C., T. Salameh, and A. Merabet (2020), 'Technico-economic Analysis of Off Grid Solar PV/Fuel Cell Energy System for Residential Community in Desert Region', *International Journal of Hydrogen Energy,* 45(20), pp.11460–70.

Guinot, B. et al. (2015), Techno-economic Study of a PV-Hydrogen-Battery Hybrid System for Off-grid Power Supply: Impact of Performances' Ageing on Optimal System Sizing and Competitiveness', *International Journal of Hydrogen Energy,* 40(1), pp.623–32.

Jahangiri, M. et al. (2019), 'Techno-Econo-Environmental Optimal Operation of Grid-Wind-Solar Electricity Generation with Hydrogen Storage System for Domestic Scale, Case Study in Chad', *International Journal of Hydrogen Energy,* 44(54), pp.28613–28.

Javed, M.S. and T. Ma (2019), 'Techno-economic Assessment of a Hybrid Solar–Wind–Battery System with Genetic Algorithm', *Energy Procedia*, 158, pp.6384–6392.

Kikuchi, Y., T. Ichikawa, M. Sugiyama, and M. Koyama (2018), 'Battery-assisted Low-cost Hydrogen Production from Solar Energy: Rational Target Setting for Future Technology Systems', *International Journal of Hydrogen Energy*, 44(3), pp.1451–65.

Li, B., P. Hu, N. Zhu, F. Lei, and L. Xing (2019), 'Performance Analysis and Optimization of a CCHP–GSHP Coupling System Based on Quantum Genetic Algorithm', *Sustainable Cities and Society,* 46, p.101408.

Li, Y.H. et al. (2020), 'An Improved Operation Strategy for CCHP System Based on High-Speed Railways Station Case Study', Energy Conversion and Management, 216, p.112936.

Loisel, R., L. Baranger, N. Chemouri, S. Spinu, and S. Pardo (2015), 'Economic Evaluation of Hybrid Off-shore Wind Power and Hydrogen Storage System', *International Journal of Hydrogen Energy,* 40(21), pp.6727–39.

Luo, X., Y. Zhu, J. Lu, and Y. Liu (2018), 'Design and Analysis of a Combined Desalination and Standalone CCHP (Combined Cooling Heating and Power) System Integrating Solar Energy Based on a Bi-level Optimization Model', *Sustainable Cities and Society*, 43, pp.166–75.

Luta, D.N. and A.K. Raji (2018), 'Decision-making Between a Grid Extension and a Rural Renewable Off-grid System with Hydrogen Generation', *International Journal of Hydrogen Energy,* 43(20), pp.9535–48.

Ma, T., H. Yang, and L. Lu (2014), 'A Feasibility Study of a Stand-alone Hybrid Solar–Wind–Battery System for a Remote Island', *Applied Energy*, 121(10), pp.149–58.

Ma, W., S. Fang, and G. Liu (2017), 'Hybrid Optimization Method and Seasonal Operation Strategy for Distributed Energy System Integrating CCHP, Photovoltaic and Ground Source Heat Pump', *Energy,* 141, 1439–55.

Mehrjerdi, H. (2020), 'Peer-to-peer Home Energy Management Incorporating Hydrogen Storage System and Solar Generating Units', *Renewable Energy*, 156(C), 183–92.

Mokhtara, C., B. Negrou, N. Settou, A. Boufferek, and Y. Yao (2020), 'Design Optimization of Grid-connected PV-Hydrogen for Energy Prosumers Considering Sector-Coupling Paradigm: Case Study of a University Building in Algeria', *International Journal of Hydrogen Energy*, October.

Obara, S. and J. Li (2020), 'Evaluation of the Introduction of a Hydrogen Supply Chain Using a Conventional Gas Pipeline–A Case Study of the Qinghai–Shanghai Hydrogen Supply Chain', *International Journal of Hydrogen Energy*, 45(58), 33846–59.

Ren, F., J. Wang, S. Zhu, and Y. Chen (2019), 'Multi-objective Optimization of Combined Cooling, Heating and Power System Integrated with Solar and Geothermal Energies', Energy Conversion and Management, 197, p.111866.

Ren, F., Z. Wei, and X. Zhai (2020), 'Multi-objective Optimization and Evaluation of Hybrid CCHP Systems for Different Building Types', *Energy,* p.215.

Romero Rodríguez, L., J.M.S. Lissén, J.S. Ramos, E.A.R. Jara, and S.A. Domínguez (2016), 'Analysis of the Economic Feasibility and Reduction of a Building's Energy Consumption and Emissions when Integrating Hybrid Solar Thermal/PV/Micro-CHP Systems', *Applied Energy*, 165, pp.828–38.

Ruiming, F. (2019), 'Multi-objective 'Optimized Operation of Integrated Energy System with Hydrogen Storage', *International Journal of Hydrogen Energy*, 44(56), pp.29409–17.

Singh, A., P. Baredar, and B. Gupta (2017), 'Techno-economic Feasibility Analysis of Hydrogen Fuel Cell and Solar Photovoltaic Hybrid Renewable Energy System for Academic Research Building', *Energy Conversion & Management*, 145(Aug.), pp.398–414.

Singh, S., P. Chauhan, and N.J. Singh (2020), 'Capacity Optimization of Grid Connected Solar/fuel Cell Energy System using Hybrid ABC-PSO Algorithm', International Journal of Hydrogen Energy, 45(16), pp.10070–88.

Sultan, H., A. Menesy, S. Kamel, A. Kourashy, S.A. Almohaimeed, and M. Abdel-Akher (2020), 'An Improved Artificial Ecosystem Optimization Algorithm for Optimal Configuration of a Hybrid PV/WT/FC Energy System', *Alexandria Engineering Journal*, 60(1), pp.1001–25.

Wang, X., Yang, M. Huang, and X. Ma (2018), 'Multi-objective Optimization of a Gas Turbine-based CCHP Combined with Solar and Compressed Air Energy Storage System', *Energy Conversion & Management,* 164, pp.93–101.

Xu, C., Y. Ke, Y. Li, H. Chu, and Y. Wu (2020), 'Data-driven Configuration Optimization of an Off-grid Wind/PV/Hydrogen System Based on Modified NSGA-II and CRITIC-TOPSIS', *Energy Conversion and Management,* 215, p.112892.

Xu, F., J. Liu, S. Lin, Q. Dai, and C. Li (2018), 'A Multi-objective Optimization Model of Hybrid Energy Storage System for Non-grid-connected Wind Power: A Case Study in China', *Energy,* 163, pp.585–603.

Yang, C., X. Wang, M. Huang, S. Ding, and X. Ma (2017), 'Design and Simulation of Gas Turbine-Based CCHP Combined with Solar and Compressed Air Energy Storage in a Hotel Building', *Energy & Buildings*, 153(Oct.), p.412–20.

Yang, G. and X. Zhai (2018), 'Optimization and Performance Analysis of Solar Hybrid CCHP Systems under Different Operation Strategies', *Applied Thermal Engineering*, 133, pp.327–40.

Yang, G. and X.Q. Zhai (2019), 'Optimal Design and Performance Analysis of Solar Hybrid CCHP System Considering Influence of Building Type and Climate Condition', *Energy,* 174, pp.647–63.

Zhang, Y., Q.S. Hua, L. Sun, and Q. Liu (2020), 'Life Cycle Optimization of Renewable Energy Systems Configuration with Hybrid Battery/Hydrogen Storage: A Comparative Study', *The Journal of Energy Storage,* 2020, 30, p.101470.

Zhang, W., A. Maleki, M. A. Rosen, and J. Liu (2019), 'Sizing a Stand-alone solar-wind-hydrogen Energy System using Weather Forecasting and a Hybrid Search Optimization Algorithm', *Energy Conversion and Management,* 180, pp.609–21.

Zheng, C.Y., J.Y. Wu, X.Q. Zhai, and R.Z. Wang (2017), 'A Novel Thermal Storage Strategy for CCHP System Based on Energy Demands and State of Storage Tank', *International Journal of Electrical Power & Energy Systems,* 85(4), pp.117–29.

Nomenclature	
AC	absorption chiller
ATC	annual total cost
CCHP	combined cooling, heating and power
CDE	carbon dioxide emission
COP	coefficient of performance
COM	hydrogen compressor
PEC	primary energy consumption
PGU	power generation unit
PEM	proton exchange membrane
PV	photovoltaic
Rec	heat recovery system
ST	solar thermal collector
Symbols	
A	area (m^2)
C	cost ($/kWh)
E	electricity (kWh)
F	fuel consumption (kWh)
G	the solar radiation intensity($kW/m^2/h$)
Q	thermal energy (kWh)
η	efficiency
P	installed capacity of equipment (kW)
Φ	equipment costs ($/kW)
$\dot{m}$	mass flow rate of hydrogen generated(kg/s)
Subscripts	
PV	photovoltaic
ST	solar thermal collector
ac	absorption chiller
b	boil
com	hydrogen compressor
e	electricity
el	electrolyser
ec	electricity chiller
grid	electricity grid
g	natural gas
H	heat load
He	heat exchanger
Pgu	power generation unit
Rec	heat recovery system